



ACADEMIC  
PRESS

Available online at [www.sciencedirect.com](http://www.sciencedirect.com)

SCIENCE @ DIRECT®

Icarus 163 (2003) 263–289

ICARUS

[www.elsevier.com/locate/icarus](http://www.elsevier.com/locate/icarus)

## Cratering rates in the outer Solar System

Kevin Zahnle,<sup>a,\*</sup> Paul Schenk,<sup>b</sup> Harold Levison,<sup>c</sup> and Luke Dones<sup>c</sup>

<sup>a</sup> NASA Ames Research Center, MS 245-3, Moffett Field, CA 94035, USA

<sup>b</sup> Lunar & Planetary Institute, Bay Area Boulevard, Houston, TX 77058, USA

<sup>c</sup> Southwest Research Institute, 1050 Walnut Street, Boulder, CO 80302, USA

Received 19 June 2002; revised 7 January 2003

### Abstract

This paper is a compilation by table, graph, and equation of impact cratering rates from Jupiter to Pluto. We use several independent constraints on the number of ecliptic comets. Together they imply that the impact rate on Jupiter by 1.5-km-diameter comets is currently  $\dot{N}(d > 1.5 \text{ km}) = 0.005_{-0.003}^{+0.006}$  per annum. Other kinds of impactors are currently unimportant on most worlds at most sizes. The size–number distribution of impactors smaller than 20 km is inferred from size–number distributions of impact craters on Europa, Ganymede, and Triton; while the size–number distribution of impacting bodies larger than 50 km is equated to the size–number distribution of Kuiper Belt objects. The gap is bridged by interpolation. It is notable that small craters on Jupiter’s moons indicate a pronounced paucity of small impactors, while small craters on Triton imply a collisional population rich in small bodies. However it is unclear whether the craters on Triton are of heliocentric or planetocentric origin. We therefore consider two cases for Saturn and beyond: a Case A in which the size–number distribution is like that inferred at Jupiter, and a Case B in which small objects obey a more nearly collisional distribution. Known craters on saturnian and uranian satellites are consistent with either case, although surface ages are much younger in Case B, especially at Saturn and Uranus. At Neptune and especially at Saturn our cratering rates are much higher than rates estimated by Shoemaker and colleagues, presumably because Shoemaker’s estimates mostly predate discovery of the Kuiper Belt. We also estimate collisional disruption rates of moons and compare these to estimates in the literature.

© 2003 Elsevier Science (USA). All rights reserved.

### 1. Introduction

This study presents a self-consistent set of primary cratering rates for the moons of the jovian planets. These rates can be compared with observed crater densities to place rough upper limits on surface ages. We emphasize the ecliptic comets (Jupiter-family comets, Centaurs, and the like), as these dominate impact cratering in the outer Solar System (Shoemaker and Wolfe, 1982; Smith et al., 1982, 1986, 1989; Zahnle et al., 1998). For completeness we also address the nearly isotropic comets (long-period comets and Halley-type comets) and the Trojan asteroids. We do not address extinct or hypothetical cratering populations.

Our method for estimating cratering rates follows from our previous study of cratering rates on the Galilean satellites (Zahnle et al., 1998; hereafter ZDL98), which in turn

was based on impact rates on the giant planets obtained by Levison and Duncan 1997; hereafter LD97) from a numerical simulation of the migration and scattering of ecliptic comets. Since then Levison et al. (2000, hereafter L0) revised their estimates of the impact rates on the giant planets downward by a factor of 4, and Bottke et al. (2002) further revised the new rate downward by another factor of 3. The older, higher impact rates were in better accord with the historical rate that comets have been observed to pass close to Jupiter (ZDL98). Meanwhile other constraints on impact rates at Jupiter have become available and these too are in better accord with the historical rate than with the Bottke et al. rates. The new constraints will be discussed in detail in the following; we list them here. Carbon monoxide is a major product of impact shock chemistry. Its abundance in the jovian stratosphere can be explained by impact rates 5–10 times higher than those recommended by Bottke et al. (Bézar et al., 2002). New crater counts on Ganymede that use Galileo data constrain the size distribution of comets

\* Corresponding author. Fax: +1-650-604-6779.

E-mail address: [kzahnle@mail.arc.nasa.gov](mailto:kzahnle@mail.arc.nasa.gov) (K. Zahnle).

with diameters less than 20 km, while Kuiper Belt surveys appear to have converged on a size distribution for large ( $d > 50$  km) objects. Given these size distributions it is possible to link the number of large Centaurs at Saturn—an independent observational constraint on the number of ecliptic comets—to the impact rate of small comets at Jupiter, with results that are consistent with the higher impact rates suggested by the historical record. Crater densities on the bright terrains of Ganymede can be used to make an independent inference of the cratering rate based on the presumption that the making of the bright terrains is linked to the existence of a dynamo-generated magnetic field. This admittedly weak constraint also implies impact rates comparable to the historic rate.

Another issue with our previous analysis is that we ignored the depletion of small comets in the inner Solar System. In ZDL98 we presumed that we could extrapolate Shoemaker and Wolfe's (1982) power-law size distribution, derived for comets with  $d > 2$  km to comets with  $d < 1$  km. It now seems clear that, at least from Jupiter inward, there are markedly fewer small comets than the extrapolation predicts (Ivanov et al., 1998). The strikingly different discovery histories of small comets and small near-Earth asteroids implies that comets much smaller than 1 km are rare near Earth (e.g., Shoemaker and Wolfe, 1982; Fernandez et al., 1999). Craters smaller than 20 km in diameter are rarer on lightly cratered surfaces on Europa, Ganymede, and Callisto than they are on the Moon (Schenk et al., 2003). Here we will use the observed crater densities on Europa and Ganymede to constrain the slope of the size–number distribution of small ecliptic comets at Jupiter. For the outer reaches of the Solar System we will also use crater counts from Triton. It is interesting to note that Triton, unlike Europa, features a typical population of small craters. But with Triton it is not clear whether we are seeing heliocentric comets or planetocentric debris (Croft et al., 1995; Schenk and Sobieszcyk, 1999; Stern and McKinnon, 2000; Zahnle et al., 2001).

In this study we will put the greatest weight on the historical record, and so we will recommend relatively high impact rates. These rates should not be taken too seriously, at least not yet. The most important caveat to remember is that the uncertainties are great, and the greatest uncertainties are in the comets themselves.

## 2. Comets and asteroids

For our first iteration we will assume that most primary impact craters in the outer Solar System are made by ecliptic comets. The ecliptic comets are a nomenclatural replacement for the short-period comets, in which the arbitrary distinction between comets on the basis of period is replaced by a more physically based distinction based on the Tisserand parameter (Levison, 1996). As the name implies, ecliptic comets are concentrated toward the plane of the

ecliptic; i.e., they revolve in prograde orbits that interact strongly with the planets. They are to be distinguished from the “nearly isotropic” long-period comets and Halley-type short-period comets that are only weakly concentrated in low-inclination prograde orbits (Levison, 1996). These distinctions reflect different degrees of flattening of the ancestral populations. A popular working model (Duncan et al., 1988; Gladman et al., 2001) has been that the ecliptic comets and the nearly isotropic comets are dynamically distinct, with the former evolving inward from the Kuiper Belt or the scattered disk, while the latter fall from the Oort cloud (outer or inner). When under Jupiter's control ecliptic comets are called Jupiter-family comets (JFCs). When between Neptune and Saturn ecliptic comets are called Centaurs.

The nearly isotropic comets (NICs) are less important than ecliptic comets at Jupiter (ZDL98), and they become progressively less important in the more distant parts of the Solar System. Asteroids from the asteroid belt are currently insignificant in the Outer Solar system (Shoemaker and Wolfe, 1982; ZDL98). Asteroids from the clouds of Trojans that lead and trail Jupiter by  $\sim 60^\circ$  might be of some importance for making very small craters at Jupiter (ZDL98). We will address the nearly isotropic comets and the Trojan asteroids in detail in Section 4.6. Secondary sources—ejecta either launched into planetocentric orbit by larger primary impacts or originating from the catastrophic disruption of small moons—are plausible and there is good evidence that they have at times been important (Smith et al., 1982, 1986; Strom, 1987; Croft et al., 1995; Alvarellos et al., 2002). We will not address secondary sources in detail here, but neither will we ignore them. We note that any additional cratering population will have the effect of making our estimated cratering rates lower limits, and our estimated surface ages, upper limits.

## 3. Cratering rates

Cratering rates are determined by the numbers and sizes of the comets; their distribution in space; their impact probabilities with the various targets; their impact velocities with those targets; and the diameter of the crater produced on the targets by impactors of known mass, velocity, and incidence angle. Of these many factors, the best determined are typical impact velocities, incidence angle, and the relative impact rates on satellites and the central planet (Table 1). The listed quantities are determined by using the Monte Carlo algorithm described by ZDL98 and Zahnle et al. (2001; hereafter Z01). This algorithm accounts for the different impact probabilities associated with different orbits, and it filters out objects that hit the planet and so are no longer available to hit the satellite. An illustrative approximation to the more complete model can be obtained from basic geometry. First, approximate the average impact velocity by

Table 1  
Cratering parameters

	$P_{EC}^a$	$g^b$	$\rho_t$	$\langle u_i \rangle^c$	$d(D = 20)^d$	$D_c^e$
Jupiter	1.00					
Metis	$2.8 \times 10^{-7}$	1.4	1.0	59	0.26	15
Amalthea	$7.7 \times 10^{-7}$	2.6	1.0	50	0.35	15
Thebe	$2.9 \times 10^{-8}$	0.6	1.0	45	0.24	15
Io	$1.4 \times 10^{-4}$	181	2.7	32	2.16	15
Europa	$6.6 \times 10^{-5}$	130	0.9	26	1.08	2.5
Ganymede	$1.2 \times 10^{-4}$	143	0.9	20	1.26	2.5
Callisto	$6.1 \times 10^{-5}$	125	0.9	15	1.26	2.5
Himalia	$1.4 \times 10^{-8}$	3.8	1.5	6.1	1.87	15
Saturn	0.42					
Prometheus	$1.7 \times 10^{-7}$	0.8	0.6	32	0.26	15
Pandora	$1.0 \times 10^{-7}$	0.7	0.6	31	0.25	15
Epimetheus	$1.8 \times 10^{-7}$	1.0	0.6	30	0.28	15
Janus	$4.5 \times 10^{-7}$	1.6	0.6	30	0.32	15
Mimas	$1.7 \times 10^{-6}$	6.5	0.9	27	0.60	15
Enceladus	$2.2 \times 10^{-6}$	8.5	0.9	24	0.69	15
Tethys	$7.9 \times 10^{-6}$	18.5	0.9	21	0.91	15
Teleso/Calypso	$3.5 \times 10^{-9}$	0.28	0.9	21	0.28	15
Dione	$7.1 \times 10^{-6}$	22.4	0.9	19	1.03	15
Helene	$5.8 \times 10^{-9}$	0.4	0.9	19	0.34	15
Rhea	$9.6 \times 10^{-6}$	28.5	0.9	16	1.21	15
Titan	$5.4 \times 10^{-5}$	135	0.9	10.5	1.79	2.5
Hyperion	$1.0 \times 10^{-7}$	4.3	0.9	9.4	0.95	15
Iapetus	$1.4 \times 10^{-6}$	24	0.9	6.1	1.96	15
Phoebe	$8.7 \times 10^{-9}$	3.7	0.9	3.2	1.66	15
Uranus	0.25					
Cordelia	$3.3 \times 10^{-8}$	0.54	0.9	20	0.35	15
Ophelia	$4.2 \times 10^{-8}$	0.63	0.9	19	0.37	15
Bianca	$8.2 \times 10^{-8}$	0.9	0.9	18	0.43	15
Cressida	$1.6 \times 10^{-7}$	1.3	0.9	18	0.48	15
Desdemona	$1.2 \times 10^{-7}$	1.1	0.9	18	0.46	15
Juliet	$3.0 \times 10^{-7}$	1.8	0.9	18	0.52	15
Portia	$4.7 \times 10^{-7}$	2.3	0.9	18	0.56	15
Rosalind	$1.3 \times 10^{-7}$	1.2	0.9	17	0.48	15
Belinda	$1.4 \times 10^{-7}$	1.4	0.9	16	0.51	15
Puck	$6.6 \times 10^{-7}$	3.2	0.9	15	0.67	15
Miranda	$5.2 \times 10^{-6}$	8.1	0.9	12.5	0.97	15
Ariel	$2.1 \times 10^{-5}$	29	0.9	10.3	1.53	15
Umbriel	$1.6 \times 10^{-5}$	22	0.9	8.7	1.57	15
Titania	$1.8 \times 10^{-5}$	36	0.9	6.8	2.05	15
Oberon	$1.3 \times 10^{-5}$	32	0.9	5.9	2.15	15
Neptune	0.27 <sup>f</sup>					
Naiad	$2.0 \times 10^{-7}$	1.1	0.9	22	0.41	15
Thalassa	$3.8 \times 10^{-7}$	1.6	0.9	22	0.45	15
Despina	$1.2 \times 10^{-6}$	2.9	0.9	21	0.54	15
Galatea	$1.2 \times 10^{-6}$	3.1	0.9	20	0.58	15
Larissa	$1.6 \times 10^{-6}$	3.8	0.9	18	0.64	15
Proteus	$4.8 \times 10^{-6}$	8.1	0.9	14	0.90	15
Triton	$7.5 \times 10^{-5}$	78	0.9	8.2	1.95	6
Nereid	$1.2 \times 10^{-7}$	6.7	0.9	2.8	2.10	15
Pluto	$2.0 \times 10^{-4}$	64	1	1.9	4.2	6
Charon	$3.2 \times 10^{-5}$	26	1	1.8	3.9	15

<sup>a</sup> Ecliptic comet impact probability relative to Jupiter.

<sup>b</sup> Surface gravity [ $\text{cm/s}^2$ ].

<sup>c</sup> Average impact velocity [ $\text{km/s}$ ].

<sup>d</sup> Comet diameter giving  $D = 20$ -km crater [ $\text{km}$ ].

<sup>e</sup> Transition crater diameter [ $\text{km}$ ].

<sup>f</sup> L0 give  $P_{EC} = 0.54$  for Neptune. We have halved this for reasons discussed in the text.

$$\langle v_i \rangle \approx \sqrt{3v_{\text{orb}}^2 + v_{\infty}^2 + v_{\text{esc}}^2} \quad (1)$$

where  $v_{\infty}$  represents the distant encounter velocity of the comet with the planet, and  $v_{\text{orb}}$  and  $v_{\text{esc}}$  represent the orbital and escape velocities of the satellite (Lissauer et al., 1988). In general  $v_{\text{orb}}$  is by far the largest term in Eq. (1), which makes  $\langle v_i \rangle$  insensitive to  $v_{\infty}$ . For the ecliptic comets  $\langle v_{\infty} \rangle \approx \sqrt{e^2 + i^2} V_{\text{orb}}$ , where  $e$  and  $i$  represent the eccentricity and inclination of the comet and  $V_{\text{orb}}$  represents the orbital velocity of the planet. In the detailed algorithm we describe  $v_{\infty}$  with a fit to the distribution of encounter velocities of JFCs with Jupiter obtained by LD97. The average of these is  $\langle v_{\infty} \rangle \approx 0.34 V_{\text{orb}}$ . The more complete Monte Carlo estimate (ZDL98) of  $\langle v_i \rangle$  is about 5% higher than  $v_i$  given by Eq. (1).

The relative impact rate on a satellite vs its planet is approximated by the ratio of the surface area of the satellite to the surface area of the sphere encompassed by its orbit, multiplied by a factor that accounts for the cumulative periape distribution of the comets as influenced by the planet's gravitational focusing,

$$\frac{N(<a)}{N(<a_s)} = \frac{v_{\infty}^2(a/a_s)^2 + 2v_{\text{orb}}^2(a/a_s)}{v_{\infty}^2 + 2v_{\text{orb}}^2} \quad (2)$$

In Eq. (2) the number of objects passing within a distance  $a$  of the planet is normalized to the total number crossing the satellite's orbit; it assumes circular orbits and neglects gravitational focusing by the satellite itself. For impacts on the planet  $a = R_p$ . The relative number of impacts on a satellite to those on the planet scales as

$$\frac{P_s}{P_p} \approx \frac{R_s^2}{a_s^2} \frac{N(<a)}{N(<a_s)} \quad (3)$$

For all but the most distant satellites,  $v_{\infty}^2 \ll 2v_{\text{orb}}^2$ , so that gravitational focusing is large, the differential periape distribution is uniform, and the cumulative distribution is proportional to the periape distance,  $N(<a_s)/N(<a) \approx a/a_s$ . There results

$$\frac{P_s}{P_p} \approx \frac{R_s^2}{a_s^2} \frac{a_s}{R_p} \quad (4)$$

Equation (4) says that Ganymede (for example) is hit  $9 \times 10^{-5}$  as often as Jupiter. The more accurate Monte Carlo estimate of  $1.2 \times 10^{-4}$  (Table 1) is about 30% higher. Equation (4) is a poorer approximation to Eq. (3) for the more distant satellites.

The spatial distribution of ecliptic cometary orbits is adapted from detailed numerical simulations of the orbital evolution of Kuiper Belt objects (LD97). Relative impact rates on the giant planets after L0 are listed in Table 1. Nakamura and Kurahashi (1998) performed a somewhat similar study, but they started with known active short-period comets; their study proved too biased for us to use.

The greatest uncertainty remains in calibrating the numbers, masses, and size distributions of the comets. There are

three main sources of information. These are the craters themselves, which furnish an integrated record of the size-number distribution of the impactors over  $10^7$ - to  $10^{10}$ -year time scales; the observed sizes and numbers of ecliptic comets, which furnish a snapshot of the currently available impactors over  $10^4$  to  $10^6$ -year time scales; and the direct and indirect observations of impacts on Jupiter, which furnish historical information on  $10^2$  to  $10^3$ -year time scales.

### 3.1. Crater scaling

We relate crater diameter  $D$  to impactor diameter  $d$  through

$$D_s = 11.9(v^2/g)^{0.217}(\rho_i/\rho)^{0.333} d^{0.783} \text{ km} \quad (5)$$

and

$$D = \begin{cases} D_s & (D_s < D_c) \\ D_s (D_s/D_c)^{\xi} & (D_s > D_c) \end{cases} \quad (6)$$

Arguments that lead to Eqs. (5) and (6) are given in the Appendix. In these expressions the diameters  $D$ ,  $D_s$ ,  $D_c$ , and  $d$  are in kilometers, the impact velocity  $v$  is in kilometers per second, and the surface gravity  $g$  is in centimeters per second squared. The diameter  $D_s$  refers to the diameter of the simple (transient) crater. The diameter  $D_c$  refers to the transition between simple and complex craters; it is an observed quantity that is in principle unique to each world. For simplicity we take  $D_c = 2.5$  km for Europa, Ganymede, Callisto, and Titan (Schenk et al., 2003);  $D_c = 6$  km for Triton and Pluto; and  $D_c = 15$  km for all other satellites. We take the power  $\xi = 0.13$  (McKinnon et al., 1991). We will assume an impactor density of  $\rho_i = 0.6 \text{ g/cm}^3$ , consistent with the density of SL9 (Asphaug and Benz, 1996). Target densities and simple-complex crater scaling parameters are listed in Table 1. Equations (5) and (6) represent a compromise between unwarranted precision and practicality. It is appropriate to discriminate between Ganymede on the one hand and Mimas (say) on the other; the differences in their craters are both relatively large and known. Otherwise any systematic errors introduced by using these expressions in place of more complicated expressions are small compared to a multitude of other systematic and stochastic errors that affect this work.

### 3.2. Apex-antapex asymmetries

Primary cratering of a synchronously rotating satellite by heliocentric comets is expected to be strongly asymmetric, with the leading hemisphere being much more quickly cratered than the trailing hemisphere (Shoemaker and Wolfe, 1982, Horedt and Neukum, 1984, Z01). A semiempirical generalization of Zahnle et al., (2001) numerical experiments is that the cratering rate  $\dot{N}$  per unit surface area for a power-law cumulative impactor size distribution  $N(>d) \propto d^{-b}$  varies as a function of the angular distance  $\beta$  from the apex of motion as

$$\dot{N} = A(1 + \cos \beta / \sqrt{2 + v_\infty^2/v_{\text{orb}}^2})^{2.0+0.47b}. \quad (7)$$

Numerical experiments indicate that Eq. (7) works well for  $1 < b < 4$  and any realistic value of  $v_\infty$ . Equation (7) can be normalized so that the total number of craters corresponds to the global average cratering rate by integrating over all  $\beta$ . The resulting normalization factor is

$$A = \frac{2\lambda\nu}{(1+\nu)^\lambda - (1-\nu)^\lambda} \quad (8)$$

where  $\lambda = 3.0 + 0.47b$  and  $\nu = 1/\sqrt{2 + v_\infty^2/v_{\text{orb}}^2}$ .

For ecliptic comets and asteroids,  $v_\infty^2 \ll v_{\text{orb}}^2$ , and so the factor multiplying  $\cos \beta$  is  $\sim\sqrt{1/2}$ . Exceptions are for the distant irregular satellites, for which  $v_{\text{orb}}$  is small, or impacts by nearly isotropic comets, for which  $v_\infty \approx \sqrt{3}V_{\text{orb}}$ . For example, for 30-km-diameter craters on Ganymede, for which data are good,  $b \approx 1.7$ , so that for ecliptic comets or asteroids

$$\dot{N} \propto (1 + 0.66 \cos \beta)^{2.8} \quad (9)$$

and  $A = 0.73$ . Production crater densities near the apex ( $\beta < 30^\circ$ ) are therefore 2.6 times higher than the global average and 3.5 times higher than at  $\beta = 90^\circ$ . The bigger effect is at the antapex, where production crater densities are reduced by a factor of 15 from the global average. The expected difference between apex and antapex cratering rates is about a factor of 40.

For nearly isotropic comets striking Ganymede,

$$\dot{N} \propto (1 + 0.4 \cos \beta)^{2.8}. \quad (10)$$

The predicted apex–antapex asymmetry is about a factor of 8.

A second relation between crater size  $D$  and apex angle  $\beta$  is needed to describe cratering rates as a function of  $\beta$ . A useful expression for ecliptic comets,

$$D(\beta) \propto (1 + 0.66 \cos \beta)^{0.43}, \quad (11)$$

is obtained for constant comet diameter  $d$  in Monte Carlo simulations for Ganymede. Equation (11) should work reasonably well for all the synchronous satellites.

In the jovian system only the younger bright terrains of Ganymede exhibit a pronounced apex–antapex cratering asymmetry (Schenk and Sobieszcyk, 1999; Z01). The observed asymmetry is about a factor of 4, which falls well short of the predicted factor of 40. One possible explanation is that we are looking at the effects of crater saturation, in the sense that younger craters are obliterating older craters (Z01). However, crater densities on the bright terrains are a fewfold lower than expected of saturation. A second possibility is that we are looking mostly at the effects of nearly isotropic comets. This is unlikely given that today the impact rate by NICs is only about 4% that of ECs (see Section 4.b). Our preferred hypothesis is that Ganymede has rotated nonsynchronously some time in the astronomically recent past. What is required is that about half the big craters on the bright terrains be attributed to a time before nonsynchro-

nous rotation stopped. Nonsynchronous rotation implies a warmer mantle, so that the ice shell can effectively decouple from the interior. This seems consistent with tidal evolution through earlier resonances, as discussed by Showman and Malhotra (1997). In the simplest story the bright terrains are all roughly the same age, although we showed that they could be of randomly different ages and not significantly dilute the apex–antapex asymmetry (Z01).

Planetocentric debris can crater symmetrically (Horedt and Neukum, 1984), but there does not appear to be a plausible source for large planetocentric objects in the jovian system. A 30-km-diameter crater on Ganymede implies a 2-km-diameter comet striking at 21 km/s, or a 5-km chunk of planetocentric debris striking at 5 km/s. There are hundreds of 30-km-diameter impact craters on Ganymede. It is difficult to put hundreds of 5-km icebergs into orbit about Jupiter. By contrast planetocentric debris are likely to be important for the satellites of Saturn and Uranus.

### 3.3. The size distribution of impactors at Jupiter

For small craters we use populations on Europa and those superposed on the young large basins Gilgamesh (on Ganymede) and Lofn (on Callisto). We invert the crater counts using Eqs. (5) and (6) to obtain the size–number distribution of small comets at Jupiter. The inversions are shown in Fig. 1. The best data are from Europa. Based on  $\sim 100$  craters with  $D > 1$  km, we infer a cumulative comet size distribution  $N(>d) \propto d^{-b}$  with  $b = 0.9$  for  $d < 1$  km. The distribution appears to steepen for  $d > 1$  km ( $D > 20$  km), but there are too few large craters for any surety in this. Crater densities superposed on Gilgamesh are much higher than on Europa, and there is consequently more reason to fear confusion or erosion or contamination by secondaries. Here we work with two counts, one for Gilgamesh as a whole and another restricted to the ejecta blanket (Schenk et al., 2003). The former has more craters at wider diameters while the latter is more representative at smaller diameters. The Gilgamesh data also hint at a steepening slope for the bigger craters, but at a larger size. Hence we suspect that the apparent steepening of the slope for the few largest craters is, at least in part, a statistical artifact. Overall we see a consistent picture of a production population that is greatly depleted of small objects compared to most other Solar System crater-forming populations. From craters on Gilgamesh, the inferred slope of the power-law distribution is  $1 < b < 1.2$  for  $d < 2$  km.

Larger craters tell a different story. Schenk and Sobieszcyk (1999) compiled a database of all craters on the mapped parts of Ganymede with  $D > 30$  km. Mapping of Ganymede at adequate resolution is 95% complete. Because the crater density is lower on the bright terrains than it is on the older dark terrains, or on Callisto, we will begin by assuming that the observed crater diameter distribution approximates a production population. If we do this we infer that for comet sizes  $2 < d < 5$  km the effective slope is  $b = 1.7$ , and for

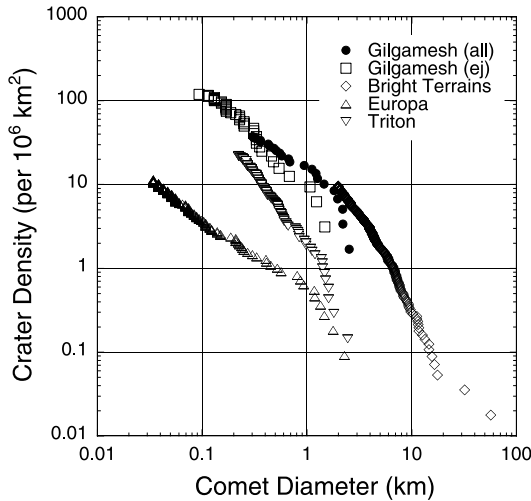


Fig. 1. The size–number distribution of impactors obtained from young surfaces in the outer Solar System. Europa had seemed remarkable for the relative dearth of small craters, which implies a corresponding dearth of small comets. But similar data are retrieved from Gilgamesh, a moderately cratered impact basin on Ganymede, and from Lofn, a somewhat comparable basin on Callisto (Schenk et al. 2003). Difficulty in recognizing small impact craters in the central parts of Gilgamesh led us to present a second count restricted to the craters on the ejecta blanket. In this way we can extend the counts to smaller craters. Also shown are comet diameters inferred from craters on the bright terrains of Ganymede for craters  $D > 30$  km. This shows that the size–number distribution steepens rapidly for bigger objects. Also shown is the much steeper size–number distribution determined for Triton.

$5 < d < 20$  km the slope is  $b \approx 2.5$ . Above this size there are but two craters. These inversions are plotted on Fig. 1.

It seems that the size distribution of comets at Jupiter steepens for  $1 < d < 2$  km, but there are too few data to define at just what size the change occurs. The change in slope at  $d \approx 5$  km (corresponding to 70-km-diameter craters) may be an artifact of saturation. But it is noteworthy that the slope of the size distribution of Kuiper Belt objects with  $d > 50$  km is apparently even steeper,  $b \approx 3.2$  (Trujillo et al., 2001, Gladman et al., 2001). A naive reading of the data shows a monotonic increase in the slope as  $d$  increases, from  $b \approx 1$  for  $d < 1$  km, rising to  $b \approx 3.2$  for  $d > 50$  km, and passing through  $b \approx 1.7$  for  $2 < d < 5$  and  $b \approx 2.5$  for  $5 < d < 20$ . Here we will fill in the gap by assuming that  $b = 1$  for  $d < 1.5$  km and  $b = 1.7$  for  $d > 1.5$  km. We call this Case A. This curve is plotted on Fig. 2, along with a great deal of other information that we will discuss in the sections that follow.

The shallow size distribution for  $d$  between about 1 and 10 km is similar to size distributions of JFCs determined by direct observations. For example, Donnison (1986) suggested that  $b = 1.4$  and Lowry et al. (2003) report that  $b = 1.6$  for  $1 < d < 15$  km. That the distribution becomes progressively steeper at larger sizes has also been suggested before (e.g., Weissman and Levison, 1997).

### 3.4. The size distribution at Triton

Triton is sparsely cratered. Saturation is not an issue. Here we use newly reprocessed Voyager images encompassing 30% of Triton’s surface to address both their size–number distribution and their spatial distribution (Schenk and Sobieszczyk, 1999; Z01). Triton’s apex–antapex asymmetry is both very large and unlike that predicted of heliocentric comets; rather, it resembles what would be produced by a population of prograde planetocentric debris striking retrograde Triton head-on. The most telling data are for apex angles  $\beta \approx 90^\circ$ , for which excellent images are available and impact craters are not seen, a distribution in  $\beta$  to be expected of head-on collisions but not of heliocentric comets. Either we are looking at a record of prograde planetocentric impactors or there has been nonrandom resurfacing of the imaged surfaces with  $\beta > 60^\circ$  that mimics planetocentric

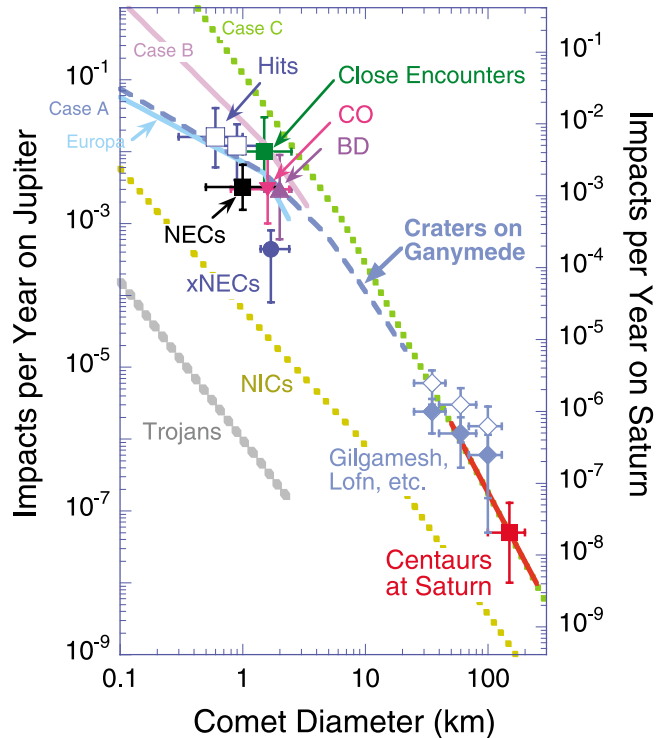


Fig. 2. Impact rates at Jupiter and Saturn. Data points refer to various estimates of the impact rate of Jupiter, with the exception of the Centaurs, which refer to the impact rate at Saturn. The data are discussed in detail in the text. The lines give the slopes of the size–frequency distributions as obtained from craters on Europa, Ganymede, and Triton (Fig. 1), and from the observed populations of Kuiper Belt objects (plotted through the Centaurs). Generous error bars are to remind the authors that uncertainties are large. Case A refers to the relative abundance of small comets at Jupiter. Case B refers to the relative abundance of small comets at Triton; this latter assumes that the craters on Triton are made by comets. Case C is representative of the expected mass distribution of small comets from a collisional Kuiper Belt. Also shown for comparison are impact rates on Jupiter by Trojan asteroids and NICs. The former is a lower limit because it considers only dynamical loss from the L4 and L5 swarms; if collisional losses are important the impact rate at Jupiter is increased proportionately.

centric cratering. Neither of these alternatives seems very likely.

For our present purposes, we need to consider both possibilities. If heliocentric, the size–number distribution of the craters reflects the size–number distribution of small comets at Neptune. It is much steeper than the comet size–number distribution at Jupiter (see Fig. 1). It is fully consistent with an evolved collisional distribution, for which  $b = 2.5$  (Dohnanyi, 1972; Safronov, 1972; Williams and Wetherill, 1994; Tanaka et al., 1996). The implication is that many small ecliptic comets vanish as they migrate from Neptune to Jupiter. The direct inversion implies that  $b \approx 1.7$  for  $d < 1.5$  km and  $b \approx 3.6$  for  $d > 1.5$  km. The change in slope is reminiscent of the changes in slope seen on Gilgamesh and Europa, but again we are dealing with small-number statistics for the largest craters, and the usual caveats apply.

Here we will make the conservative assumption that the slope deduced at Ganymede for  $5 < d < 20$  km extends to  $d = 1.5$  km at Triton, so that  $b \approx 2.5$  for  $1.5 < d < 20$  km. What makes this conservative is that we are invoking the smallest number of vanishing comets (comets with  $d > 5$  km are treated as indestructible). This gives the fewest comets, given the presumption that the tritonian craters are heliocentric. This distribution we call Case B. It too is plotted on Fig. 2.

If Triton’s craters have a planetocentric source, the size–number distribution of the craters tells us nothing about the comets at Neptune. Instead it gives us the size–number distribution of the planetocentric debris. In this particular case the inversion gives roughly the same diameters as for heliocentric comets, because typical impact velocities are similar,  $2v_{\text{orb}}$  for head-on impacts vs  $\sim \sqrt{3}v_{\text{orb}}$  for heliocentric comets.

#### 4. Absolute cratering rates

There are several independent ways of estimating cratering rates at Jupiter.

##### 4.1. The onset of the dynamo

The most direct but least convincing constraints on cratering rates are based on the craters themselves and presumptions about the secular cooling of Ganymede. The simplest of these is to presume that the bright terrains are younger than 4.5 Gyr. The observed average density of 30-km (diameter) impact craters on bright terrains on Ganymede is  $N(>30 \text{ km}) = 10$  per  $10^6 \text{ km}^2$ . The typical 30-km crater on Ganymede is made by a  $d = 2.0 \pm 0.5$  km diameter comet. Using  $1.2 \times 10^{-4}$  as the ratio of global impact rates on Ganymede to Jupiter (Table 1), the average rate that  $d \geq 2.0$  km comets struck Jupiter over the past 4 Gyr would be  $2 \times 10^{-3}$  per year. If it is further presumed that the impact rate has declined as  $t^{-1}$  (Holman and Wis-

dom, 1993), the current impact rate reduces to  $8 \times 10^{-4}$  per year for  $d \geq 2.0$  km. These are lower limits because the bright terrains need not be 4-Gyrs old.

A more speculative argument begins with the assumption that Ganymede’s magnetic dynamo is relatively young. Such a dynamo endures only while the conducting fluid core cools fast enough to convect (Showman and Malhotra, 1997; Spohn and Breuer, 1998). Without a heat source the expected cooling time scale is less than a billion years (Spohn and Breuer, 1998), a time scale consistent with the apparent early collapse of the martian magnetic field (Stevenson, 2001). If the ganymede dynamo awoke because the mantle began to cool after an episode of tidal heating, one might equate the onset of the dynamo to the end of nonsynchronous rotation. Here we will lump these time scales together as the magnetic dynamo time scale, which we denote  $T_{\text{BD}} < 1$  Gyr. About half of the impact craters on the bright terrains postdate synchronicity (Z01). From all this we infer that  $d = 2.0$  km comets currently strike Jupiter at a rate of  $\sim 4 \times 10^{-3}$  ( $1 \text{ Gyr}/T_{\text{BD}}$ ) per annum.

Given these considerations, we will take the crater density on the bright terrains of Ganymede to imply an annual impact rate of  $d = 2.0 \pm 0.5$  km comets on Jupiter of  $3_{-2.5}^{+9} \times 10^{-3}$ . This point is plotted as “BD” on Fig. 2.

##### 4.2. The current number of ecliptic comets

The population of ecliptic comets can be inferred from any of (a) the number of small comets observed near the Earth, (b) the historical record of small comets known to have closely encountered Jupiter, or (c) the observed number of Centaurs in the more distant Solar System. We will consider all three.

In modeling the migration of ecliptic comets, LD97 assumed a dynamically cold (low inclination, low eccentricity) Kuiper Belt source. Nearly all of their test particles had initial values of  $e = 0.05$  and  $i \leq 0.2$ . It now appears that (a) the Kuiper Belt is dynamically hotter than LD97 assumed and that (b) ecliptic comets can also come from the scattered disk, a dynamically distinct population scattered into their present orbits from their origins among the planets (Duncan and Levison, 1997). LD97 did include two hotter families of particles, both Plutinos, with initial  $e = 0.2$  and  $i = 0.4$ . About the same fraction of these reached Jupiter as from the other families of test particles. From this they concluded that, as more planets are crossed, the initial conditions are less well remembered. If so, we can be reasonably comfortable with the orbital distribution of test particles at Saturn and Jupiter, and we may regard LD97’s ratio of impacts on Jupiter to those on Saturn, 0.4, as moderately secure.

##### Active and inactive near-Earth comets

Levison and Duncan (LD97) modeled the evolution of test particles from sources in the Kuiper Belt. About 30% of

the test particles spent some time as JFCs with  $q \leq 2.5$  AU. Eventually most (97%) of them either were ejected from the Solar System or were thrown into long-period orbits. The rest hit planets or the Sun. By comparing the orbits of test particles to the observed orbits of active JFCs with  $q \leq 2.5$  AU, LD97 found that the active comets were dynamically younger than the population of test particles as a whole. Under the assumption that all JFCs younger than 12,000 years are active, and all those older are inactive, they inferred that the ratio of inactive to active JFCs with  $q < 2.5$  AU lies between 2 and 7, with a best fit of 3.5. For comparison, Shoemaker et al. (1994) estimated the ratio of inactive to active comets to be 20.

To make use of LD97's simulations one must calibrate the number of ecliptic comets to some known subset of the whole population. The obvious choice is to use comets that approach the Earth. This is the approach used by LD97 and L0. The advantage of this approach is that the inventory of Earth-approaching active comets is reasonably complete; disadvantages are that a large correction must be made for inactive comets and that a leading cause of removal of comets from the population of comets is disintegration. If nearby comets are rarer than test particles in Earth-approaching orbits, the number of distant comets would be underestimated proportionately.

Based on the number (they used 40) of active JFCs with perihelia  $q < 2$  AU, L0 estimated an impact rate on Jupiter of  $6.5 \times 10^{-4}$  per year for comets of a size corresponding to active comets brighter than  $H_T = 9$ . The magnitude  $H_T$  is supposed to measure the absolute total magnitude of an active comet with coma. There is probably some relationship between  $H_T$  and a comet's true size, although authorities differ in what this relationship is [e.g., Hughes (1988), Weissman (1991), Rahe et al. (1994), Bailey et al. (1994), and Nakamura and Yoshikawa (1995) among them use four different formulations that differ by an order of magnitude in mass for kilometer-size comets]. L0 multiply their rate by a scaling factor  $S = 5$  to obtain an impact rate of  $\dot{N}_J(d > 1 \text{ km}) = 3.3 \times 10^{-3}$  per annum, but with a quoted uncertainty of "at least an order of magnitude." This point is plotted on Fig. 2 as "NECs."

Bottke et al. (2002) update this argument by using observations of inactive comets obtained from their analysis of discovery rates in the automated Spacewatch Near Earth Object survey. The approach is promising because (a) the sizes are much better constrained and (b) according to LD97 most JFCs should be inactive. Spacewatch has discovered five previously unknown and one previously known asteroid in JFC-like orbits with  $q < 1.3$  AU and  $H < 18$ . Here  $H$  is the conventional measure of an asteroid's absolute magnitude. For an albedo of  $0.04 \pm 0.02$ ,  $H = 18$  corresponds to  $d = 1.7_{-0.3}^{+0.7}$  km. From these six objects Bottke et al. deduce that there are currently  $61 \pm 50$  dormant JFCs with  $H < 18$  and that L0's parameter  $S = 1.7 \pm 1.4$ . The discussion here implies an impact rate on Jupiter of  $\dot{N}_J(d > 1.7_{-0.3}^{+0.7}) = 4.4$

$\pm 3.6 \times 10^{-4}$  per annum. This point is plotted on Fig. 2 as "xNECs."

Bottke et al. point out that their argument makes the extreme assumption that 100% of JFCs fade rather than disintegrate, and so gives a lower limit. (Disintegrations raise the inferred impact rate at Jupiter by depleting the number of objects near the Sun.) Another possible systematic bias is that their argument, like LD97's before them, does not account for comets such as P/Encke and near-Earth objects such as 3200 Phaethon that have Tisserand parameters with respect to Jupiter that are greater than 3. ZDL98 argued that neglect of P/Encke was not statistically important for impacts on Jupiter by the JFCs as a whole, as there is but one Encke out of 150 JFCs. Such objects are over-represented among near-Earth objects, an apparent endurance that implies a less enduring nature for the typical JFC.

### *The historical record*

An independent approach exploits the historical record of comets observed to make close approaches to Jupiter. One might expect such a sample to be incomplete, and the deduced rate a lower limit. What makes this confounding is that this is the highest estimate that we will make.

As discussed in ZDL98, four close encounters with Jupiter have been observed in the past 150 years. These were by P/Brooks 2 ( $2.0R_J$  in 1886), P/Gehrels 3 ( $3.0R_J$  in 1970), and D/Shoemaker–Levy 9 (SL9) ( $1.3R_J$  in 1992 and  $0.5 R_J$  in 1994). Both P/Brooks 2 and D/Shoemaker–Levy 9 were tidally disrupted into several discrete fragments. We overlooked an earlier encounter by P/Lexell, which according to computation passed within  $\sim 2.8R_J$  in 1779, nine years after it passed near the Earth as a 1st magnitude comet (Kronk, 1984, 2001). Tabe et al. (1997) have found evidence of what appears to have been an earlier close approach observed by Cassini in 1690. What Cassini saw and monitored over two weeks was a spot near the equator that closely resembled an SL9 impact feature. Tabe et al. (1997) show using modern equatorial windfields that the observed evolution of Cassini's spot quantitatively and qualitatively agrees with the evolution of a windblown SL9-like impact feature. Tabe et al. rank the 1690 event with the middle-ranking SL9 events. By our reckoning this would make it a 600-m object, comparable in size to the smallest known comets. We will count this a JFC, although there is a small chance that it was another kind of comet or an asteroid. The close approaches are collected in Table 2. We focus on close encounters because tidal interactions with Jupiter seem to freshen comets—more distant encounters would be more easily overlooked.

As the distribution of perijove distances of JFCs making close encounters with Jupiter is uniform, we can estimate how frequently Jupiter is hit by exploiting the six close encounters,

$$P_J > \frac{6 \text{ encounters}}{350 \text{ years}} \times \frac{1R_J}{4R_J} \approx 5 \times 10^{-3} \text{ year}^{-1}. \quad (12)$$

Table 2  
Famous perijoves 2003

Year	Comet	Distance ( $R_J$ ) <sup>a</sup>	Diameter [km]	Comments
1994	Shoemaker–Levy 9	0.5	1.0	Fragment L
1992	Shoemaker–Levy 9	1.3	1.5	Tidally split, 20 fragments
1970	Gehrels 3	3	3–4	D-type asteroidal spectrum
1886	Brooks 2	2.0	0.8–3.4	Tidally split, 5 fragments
1779	Lexell	2.8	2?	Discovered 1770. Ejected
1690	Cassini <sup>a</sup>	<1	0.6	A spot on Jupiter

<sup>a</sup> In most cases computed by orbital integration.

We have made several conservative assumptions in evaluating Eq. (12). By arbitrarily setting the outer distance on close approaches at  $4R_J$ , we allow for some uncertainty in the reconstruction of the orbits, although the six known close encounters all appear to have been well within that distance. A second point is that the historical roster of observed close encounters with Jupiter is biased in favor of comets that passed through the inner Solar System. Nor can we expect anything approaching 100% coverage of jovian atmospheric features in the 17th, 18th or even 19th-centuries. Last, Eq. (12) uses the longest possible time line, going back to the first telescopes and first observers even capable of seeing such events, and treating them as if they are complete.

The other issue to address is the size of these comets. Active magnitudes are more than usually misleading because the near encounters seem to have made both P/Brooks 2 and D/Shoemaker–Levy 9 quite a bit brighter than before or since, while P/Lexell, albeit a brilliant comet, passed very near the Earth and may have been in its first circuit through the inner Solar System. In its 1992 encounter with Jupiter SL9 had a diameter of 1.5–1.8 km (Asphaug and Benz, 1996), and in 1994 the largest fragments were roughly 1 km in diameter (Zahnle, 1996). Whether SL9 should be counted once, twice, or 20 times is open to debate, but Kary and Dones (1996) did show through dynamical simulations that only one time in 50 does a comet caught in temporary orbit about Jupiter make successive close encounters terminating in a collision. Scotti (1998) observed P/Gehrels 3 to have the reflectance spectrum of a D-type asteroid, which makes the deduced diameter [3 km according to Scotti, 4 km according to Tancredi et al. (2001)] seem sound. Sekanina and Yeomans (1985) estimated that the surviving (largest?) fragment of P/Brooks II is 0.8 km in diameter. This estimate predates the modern realization that comets are black. More recently, Tancredi et al. (2000) estimated that P/Brooks II is 3.4 km in diameter. P/Lexell's nominal diameter, based on its absolute magnitude (i.e.,  $H_T$ ) when closest to Earth, would be  $\sim 2$  km, but this estimate cannot be taken too seriously, and it may well have been smaller.

A better way to estimate the cumulative impact rate is to count the four comets larger than 1.5 km, taking into account that P/Gehrels 3 could not have been discovered before 1950 (at magnitude 17, P/Gehrels 3 was discovered

with the 48-inch Schmidt); the 1992 encounter by D/SL9 would not have been detected before 1900 (the comet was 14th magnitude, and no comet this faint was discovered before 1910), P/Brooks 2 (8th magnitude) would not have been discovered before 1770, nor would observational data have usefully constrained P/Lexell's orbit before 1570. Scaling using the same arbitrary  $q < 4R_J$  perijove cutoff already used, we estimate that the cumulative impact rate on Jupiter is  $\dot{N}_J(>1.5 \text{ km}) \approx 0.01$  per year, with an uncertainty of about a factor of 3.

We plot the impact rate on Jupiter consistent with the known historic close encounters on Fig. 2. The rate is plotted at  $10_{-7}^{+20} \times 10^{-3} \text{ year}^{-1}$  at a nominal diameter of  $d = 1.5_{-0.5}^{+1.0} \text{ km}$ . These rates are substantially higher than we deduced from active Earth-approaching JFCs. They are equivalent to taking  $S = 25$ . Even if one discounts Cassini (the man), and refuses to count SL9 twice, we are still left looking at four close encounters by otherwise unextraordinary comets since the origin of comet hunting 250 years ago, which corresponds to an unweighted impact rate of at least one hit per 200 years. Obviously this line of reasoning is hostage to small-number statistics, but equally obvious is that not every close encounter with Jupiter that has occurred over the past three centuries has been caught.

#### Direct hits

A second historical argument exploits the failure of modern observers to see other SL9-like events. This argument cuts the other way, putting an upper limit on small comets. The only probable observation of an impact-generated feature on Jupiter previous to SL9 was the aforementioned transient spot documented and mapped by Cassini in 1690 (Tabe et al., 1997). The general belief among Jupiter watchers is that middling SL9 events are obvious to the serious visual observer. We will therefore presume that had such an event occurred after some point in time, it probably would have been seen.

The Great Red Spot (GRS) was discovered as a feature in 1869 (Rogers, 1995). Cassini had recorded a permanent spot at the latitude of the GRS during his decades of observing Jupiter, but there is no evidence that the spot he observed was the same as the spot that was first recorded in 1869 and monitored continuously since. If it was the same spot, its

failure to be seen before 1869 speaks volumes about the quality and continuity of earlier observations of Jupiter.

The other issue is the continuity of observational coverage since 1869. Clearly Jupiter is not easily observed during the months nearest conjunction. Observations while Jupiter is a morning star are always fewer than during the more convenient evening apparitions. An impact on the 10–20% of the planet nearest the poles would be hard to see and unlikely to be reported. Overall, it is hard to see how coverage can have been much better than 50% during the 133 years since 1869. Here we note that there has been only one observed hit (SL9) in the ~66-year cumulative baseline. In our opinion it is unlikely that SL9-scale impacts as frequent as four per century would all have been missed. So we take the historical record of direct hits as implying that there are  $0.016_{-0.01}^{+0.024}$  hits per annum with  $d > 0.6_{-0.3}^{+0.4}$  km. This is the leftmost of two points plotted on Fig. 2 as “Hits.”

Rogers (1996) independently surveys all observations of Jupiter since 1878, and concludes that “no impact on the scale of SL9 fragments G, K, or L has ever been observed before, and the frequency of such impacts (allowing for unobservability during solar conjunction) is less than one per 80 years.” This would correspond to an upper limit of 0.012 hits per annum with  $d > 0.9_{-0.3}^{+0.5}$  km. This is the other point plotted on Fig. 2 as “Hits.”

#### *Carbon monoxide*

Comet impacts on Jupiter generate amounts of carbon monoxide that rival the mass of the comet. SL9 itself produced  $\sim 7 \times 10^{14}$  g of CO from a  $\sim 1 \times 10^{15}$  g comet (Harrington et al., 2003). The CO is injected at very high altitudes (Lellouch et al., 1997). Carbon monoxide is nearly inert in the jovian stratosphere. Excess CO is removed only by mixing into the troposphere. This takes time. Bézard et al. (2002) estimate that the characteristic time scale for removing CO from the jovian stratosphere is 300 years. What makes this interesting is that there appears to be substantially more excess CO in the jovian stratosphere than can be accounted for by SL9. The excess CO has a different distribution in altitude and latitude than do the shorter lived SL9 products such as CO<sub>2</sub>. The excess CO is estimated to be  $\sim (1.5 \pm 0.9) \times 10^{15}$  g, or roughly twice what was generated by SL9 (Lellouch et al., 1997).

Bézard et al. (2002) suggest that a good explanation for excess CO on Jupiter would be earlier cometary impacts, comparable to SL9, with memories persisting on the characteristic 300-year stratospheric mixing time scale. Bézard et al. (2002) tentatively reject their own hypothesis because impact rates at Jupiter suggested by Bottke et al. (2002) are 5–10 times smaller than what the hypothesis requires. Here let us reverse the argument and presume that Bézard et al. are right, and ask what impact rate is required to generate the excess CO. We can relate the total mass in a power-law distribution  $N(>m) \propto m^{-\gamma}$  to the mass of the largest single object in the distribution  $m_{\max}$  by (Tremaine and Dones, 1993)

$$M/m_{\max} = 1/(1 - \gamma), \quad (13)$$

where the right-hand side gives the mean value of the ratio and  $0 < \gamma < 1$ . By definition, one impact of mass  $m_{\max}$  occurs on the 300-year mixing time scale. The excess stratospheric CO corresponds to  $M \approx 2 \times 10^{15}$  g of impactors. From craters on Europa and Gilgamesh we have  $0.9 < b < 1.2$  for small (recent) impactors and therefore  $\gamma = b/3 \approx 0.3$ – $0.4$  for the sizes of interest. It follows that for impactors of density  $\rho = 0.6$  g/cm<sup>3</sup>, the diameter of the 300-year impactor is 1.6 km, i.e., an SL9-size event. The resulting impact rate is  $3_{-2}^{+6} \times 10^{-3}$  per annum for  $d = 1.6$  km (50% higher if we include SL9 itself, as we should have). This rate is consistent with the previously given historical rate. The (mostly stochastic) error associated with this estimate is about a factor of 2 in diameter. The point is plotted on Fig. 2 as “CO.”

#### *The Centaurs and the Kuiper Belt*

A third independent approach is to calibrate to the Centaurs. Some of these are big enough to be discovered in modest numbers beyond the orbit of Saturn. It is just now becoming possible to link these large objects to the smaller objects that are responsible for Ganymede’s largest craters.

There are three large Centaurs in Saturn-crossing orbits: Chiron, Pholus, and the lost 1995 SN55. All appear to be roughly 150–180 km in diameter (Fernandez et al., 2002). Their annual Öpik impact probabilities with Saturn are  $1.5 \times 10^{-8}$ ,  $1.0 \times 10^{-9}$ , and  $3.5 \times 10^{-9}$ , respectively. Added together they imply that 150-km objects hit Saturn at a rate of  $2 \times 10^{-8}$  year<sup>-1</sup>. To scale this impact rate to Jupiter we use L0’s Saturn/Jupiter impact ratio (0.4). It is too soon to know if the roster of big Saturn-crossing Centaurs is complete. Here we will simply plot the point labeled “Centaurs” at  $d = 150$  km on Fig. 2.

To extend this datum to smaller sizes requires a size distribution. Here surveys of Kuiper Belt objects are useful, as the objects in question are large, and the two competing groups seem to have reached a consensus. Trujillo et al. (2001) determine a cumulative slope  $b = 3_{-0.5}^{+0.6}$  for  $d > 100$  km, while Gladman et al. (2001) recommend a cumulative slope  $b = 3.4_{-0.3}^{+0.3}$  for  $d > 50$  km. Sheppard et al. (2000) argue that the same size distribution that holds for Kuiper Belt objects holds for Centaurs as well. Here we will take the average and use  $b = 3.2$ . This slope is similar to that recommended by Weissman and Levison (1997). We extend the slope to diameters as small as  $d = 50$  km. This slope is drawn through the Centaurs on Fig. 2 and is used by both Cases A and B.

#### *4.3. A few big craters*

The age of the Solar System provides a weak constraint on the frequency of the largest impacts. In particular, the impacts that created the relatively young big basins on Ganymede and Callisto are rare events. Gilgamesh has a

diameter of  $\sim 590$  km. It was formed by a  $\sim 60$ -km-diameter comet (or 40-km asteroid). The next largest young basin on Ganymede, with diameter  $\sim 350$  km, is found near the south pole ( $\beta = 98^\circ$ ) on bright terrain and has been nameless. It requires a  $\sim 30$ -km comet. Callisto also has two large young basins. Lofn (Greeley et al., 2001; Moore et al., 2002), at 355 km, can be attributed to a  $\sim 35$ -km comet. Valhalla, at  $\sim 1000$  km, is the product of a  $\sim 100$ -km comet. Valhalla is more heavily cratered than Lofn or Gilgamesh, but it is near the apex of motion, where cratering rates are especially high. It may be relatively young. Thus on Ganymede and Callisto there are four young impacts with  $d > 30$  km. Together, Ganymede and Callisto are struck  $1.8 \times 10^{-4}$  as often as Jupiter (Table 1). Spread over 4 Gyr these four impacts imply an impact rate on Jupiter of  $\dot{N}(d > 35 \pm 10 \text{ km}) = (6 \pm 3) \times 10^{-6} \text{ year}^{-1}$ . A flux declining as  $t^{-1}$  would reduce the current rate by a factor of 2.5. The higher and lower rates are both plotted on Fig. 2 with different symbols. Similar rates can be deduced for the two comets with  $d > 60$  km and the one comet with  $d \approx 100$  km. These are also plotted on Fig. 2 at  $\dot{N}(d > 60 \pm 15 \text{ km}) = (3 \pm 2) \times 10^{-6} \text{ year}^{-1}$  and  $\dot{N}(d > 100 \pm 30 \text{ km}) = (1.5 \pm 1.5) \times 10^{-6} \text{ year}^{-1}$ , respectively.

#### 4.4. Discussion

We have presented several independent estimates of the impact rate at Jupiter. Most of these are in broad agreement, although the historical record is a bit high and L0 a bit low. The one that really stands out is Bottke et al.'s estimate based on the number of inactive JFCs with perihelia near the Earth (the "xNECs"). This estimate is almost 10 times lower than the mean of the others. The discrepancy requires some discussion. The likeliest resolutions are that (a) comets are bigger than LO and Bottke et al. (2002) assumed, (b) LD97 underestimated the number of JFCs, or (c) LD97, L0, and Bottke et al. underestimated the number of inactive comets. All are possible.

Bottke et al. (2002) restricted discussion to inactive JFCs with  $q < 1.3$  AU. This is a good starting point for discussion. Consider the roster of all known JFCs that now have or ever have had  $q < 1.3$ . There have been 36 such JFCs known to date (March 2002). All were discovered after the invention of comet hunting 250 years ago. Of these 36, 15 are extant, intact, and periodic (the latter term means that they have been recovered at least once). Six are recently discovered objects whose durabilities have yet to be tested. The other 15 have suffered many fates. Only one (P/Lexell) has been scattered out of the JFC class into a distant orbit. The inferred time scale from this one ejection is  $36 \times 250 = 9000$  years, which can be compared to LD97's estimate of a 45,000-year dynamical lifetime of JFCs with  $q < 2.5$  AU. Three other JFCs have been lightly scattered into  $q > 1.3$  AU orbits (P/d'Arrest, P/de Vico-Swift, and P/Churyumov-Gerasimenko) but remain nearby. One has disinte-

grated (D/Biela) and another appears to have done so (D/Barnard 1), while two others are currently disintegrating (P/Schwassmann-Wachmann 3 and P/Machholz 2). The one with the smallest perihelion distance of them all apparently evaporated on its first apparition (D/Helfenzrieder). Two others have faded away, having given all the symptoms of evaporating (D/Brorsen and D/Gale). Two had good orbits but have not been recovered (D/Denning and D/Haneda-Campos); two others seem to have been irretrievably lost without prejudice (D/Swift and D/Blanpain). Good references for the histories of the comets are Kronk (1984, 2001, 2003).

What seems self-evident from this anecdotal survey is that, for this fiducial population, extinction or disintegration occurs more frequently than does dynamical loss. If the real loss processes in the inner Solar System are faster than the dynamical loss processes, it follows that LD97 and LO may have underestimated the total number of JFCs by the same factor.

Let us address this in more detail. In a steady-state balance of test particles we would expect as many new comets to be scattered into the population with  $q < 1.3$  AU as leave it. For test particles the loss rate is the rate that comets are scattered out: 4 out of 30 per 250 years. We will leave the six new comets out of the discussion. Therefore the lifetime of  $q < 1.3$  JFCs against scattering is  $\sim 2000$  years. For JFCs the loss rate has been higher: In addition to the scattered four, at least three have disintegrated and at least two others are disintegrating, another two have either evaporated or wholly faded, and two others have probably faded. The net effect is that the steady-state population with  $q < 1.3$  AU is roughly 4/13 of what it would be for test particles, for which scattering is the only loss. By calibrating to objects with  $q < 1.3$  AU, the number of test particles corresponding to active JFCs is underestimated by a factor of 13/4. We expect that the same sort of issues affect all active comets and that a similar balance to similar effect would apply for  $q < 2$  AU.

As already mentioned, LD97 calibrated their test particle survey to active comets with  $q < 2$  AU. In their calibration there are  $\sim 10$  active objects with  $H_T < 9$  and  $q < 1.3$  AU. We note that there are currently  $\sim 23$  active JFCs with  $q < 1.3$  AU (see earlier discussion and also Fernandez et al., 1999). When combined with the factor 4/13 incompleteness estimated here, LO's raw impact rate on Jupiter scales up from  $6.5 \times 10^{-4}$  to  $5 \times 10^{-3}$  per annum for JFCs. This estimate does not address the size of the comets, but it is directly comparable to what we have called the historical rate (Eq. (12)) which also treats comets simply as comets. The two rates also happen to be equal.

#### 4.5. Summary of cratering rates

We use two expressions, Case A based on comet sizes at Jupiter,

$$\dot{N}_A(>d) = \begin{cases} \dot{N}_J(>1.5 \text{ km}) \left(\frac{d}{1.5}\right)^{-1.0} & (d < 1.5 \text{ km}) \\ \dot{N}_J(>1.5 \text{ km}) \left(\frac{d}{1.5}\right)^{-1.7} & (1.5 < d < 5 \text{ km}) \\ \dot{N}_J(>1.5 \text{ km}) \left(\frac{1.5}{5}\right)^{1.7} \left(\frac{d}{5}\right)^{-2.5} = 0.129\dot{N}_J(>1.5 \text{ km}) \left(\frac{d}{5}\right)^{-2.5} & (5 < d < 30 \text{ km}) \\ \dot{N}_J(>1.5 \text{ km}) \left(\frac{1.5}{5}\right)^{1.7} \left(\frac{5}{30}\right)^{2.5} \left(\frac{d}{30}\right)^{-3.2} = 0.00146\dot{N}_J(>1.5 \text{ km}) \left(\frac{d}{30}\right)^{-3.2} & (d > 30 \text{ km}) \end{cases}, \quad (14)$$

and Case B based on comet sizes at Triton (subject to the caveats previously listed),

$$\dot{N}_B(>d) = \begin{cases} \dot{N}_J(>1.5 \text{ km}) \left(\frac{5}{1.5}\right)^{0.8} \left(\frac{d}{1.5}\right)^{-1.7} = 2.62\dot{N}_J(>1.5 \text{ km}) \left(\frac{d}{1.5}\right)^{-1.7} & (d < 1.5 \text{ km}) \\ \dot{N}_J(>1.5 \text{ km}) \left(\frac{1.5}{5}\right)^{1.7} \left(\frac{d}{5}\right)^{-2.5} = 0.129\dot{N}_J(>1.5 \text{ km}) (d/5)^{-2.5} & (1.5 < d < 30 \text{ km}) \\ \dot{N}_J(>1.5 \text{ km}) \left(\frac{1.5}{5}\right)^{1.7} \left(\frac{5}{30}\right)^{2.5} \left(\frac{d}{30}\right)^{-3.2} = 0.00146\dot{N}_J(>1.5 \text{ km}) \left(\frac{d}{30}\right)^{-3.2} & (d > 30 \text{ km}) \end{cases}. \quad (15)$$

Case A is calibrated to an impact rate on Jupiter of  $\dot{N}_J(>1.5 \text{ km}) = 0.005$  per annum. Case B is calibrated to Case A for comets with  $d > 5 \text{ km}$ . For cratering rates at Jupiter we use only Case A. For impact rates elsewhere we use both.

We briefly consider as Case C a fully collisional distribution for small Kuiper Belt objects. Such a distribution is popular in theoretical accounts of the origin of the Kuiper Belt (Stern, 1995, Kenyon, 2002). Case C as plotted on Fig. 2 is described by

$$\dot{N}_C(>d) = \begin{cases} \dot{N}_J(>1.5 \text{ km}) \left(\frac{1.5}{5}\right)^{1.7} \left(\frac{5}{30}\right)^{2.5} \left(\frac{30}{6.3}\right)^{3.2} \left(\frac{d}{6.3}\right)^{-2.5} = 0.216\dot{N}_J(>1.5 \text{ km}) \left(\frac{d}{6.3}\right)^{-2.5} & (d < 6.3 \text{ km}) \\ \dot{N}_J(>1.5 \text{ km}) \left(\frac{1.5}{5}\right)^{1.7} \left(\frac{5}{30}\right)^{2.5} \left(\frac{d}{30}\right)^{-3.2} = 0.00146\dot{N}_J(>1.5 \text{ km}) \left(\frac{d}{30}\right)^{-3.2} & (d > 6.3 \text{ km}) \end{cases}. \quad (16)$$

At  $d = 1.5 \text{ km}$  there are about 8 times more Case C than Case A comets; at  $d \approx 0.3 \text{ km}$  the difference is a factor of 100. If all these Case C objects exist in the Kuiper Belt, about 87% of the 1.5-km comets vanish before they reach Jupiter, and 99% of the 300-m comets vanish before they reach Jupiter.

We have chosen to use cumulative distributions rather than differential distributions because they are more directly compared with data and the statistics are better. To convert observations into a differential distribution requires not just calibrating the size scale but numerically differentiating the size scale. This is practical for crater diameters, but it is impractical for comet diameters, which are very poorly known. The disadvantage of stitching together power laws to make a cumulative distribution is that at each stitch the differential distribution is discontinuous, which is wrong. For our present purposes this is not a serious shortcoming, because we do not use the differential distributions.

Global cratering rates are obtained from Eq. (14) using the generalized expression

$$\dot{C}(>D) = P_{\text{EC}}\dot{N}\{d(D)\}, \quad (17)$$

where the factors  $P_{\text{EC}}$  are listed in Table 1, and  $d(D)$  is obtained by inverting Eqs. (5) and (6).

To address the apex angle  $\beta$  introduces considerable complexity. Equations (7) and (8) give the normalized variation in cratering rate across the surface as a function of  $\beta$  and  $b$ . These are multiplicative factors that enter on the right-hand side of Eq. (17). In addition, one needs to account for the complexity of the comet size distribution. Because impact velocities are systematically lower on the trailing hemisphere than on the leading hemisphere, a 1.5-km comet will produce a smaller crater on the trailing hemisphere. Hence the crater size corresponding to a  $d = 1.5 \text{ km}$  comet varies as a function of  $\beta$ . We use Eq. (11) to account for this effect. The complete final expressions for Case A cratering rates become

$$\dot{C}_A(\beta)(>D) = \begin{cases} 0.78B^{2.47} P_{EC}\dot{N}_J(>1.5 \text{ km}) (d(D)/1.5)^{-1} & (D < B^{0.43}D(1.5)) \\ 0.73B^{2.8} P_{EC}\dot{N}_J(>1.5 \text{ km}) (d(D)/1.5)^{-1.7} & (B^{0.43}D(1.5) < D < B^{0.43}D(5)) \\ 0.084B^{3.2} P_{EC}\dot{N}_J(>1.5 \text{ km}) (d(D)/5)^{-2.5} & (B^{0.43}D(5) < D < B^{0.43}D(30)) \\ 8.6 \times 10^{-4} B^{3.5} P_{EC}\dot{N}_J(<1.5 \text{ km}) (d(D)/30)^{-3.2} & (D < B^{0.43}D(30)) \end{cases}, \quad (18)$$

where  $B = (1 + 0.66 \cos \beta)$ . The corresponding expressions for Case B cratering rates become

$$\dot{C}_B(\beta)(>D) = \begin{cases} 2.0B^{2.8} P_{EC}\dot{N}_J(>1.5 \text{ km}) (d(D)/1.5)^{-1.7} & (D < B^{0.43}D(1.5)) \\ 0.084B^{3.2} P_{EC}\dot{N}_J(<1.5 \text{ km}) (d(D)/5)^{-2.5} & (B^{0.43}D(1.5) < D < B^{0.43}D(30)) \\ 8.6 \times 10^{-4} B^{3.5} P_{EC}\dot{N}_J(<1.5 \text{ km}) (d(D)/30)^{-3.2} & (D > B^{0.43}D(30)) \end{cases}. \quad (19)$$

These expressions can be used to describe local cratering rates on synchronously rotating satellites.

#### 4.6. Nearly isotropic comets

Nearly isotropic comets are divided between Oort cloud (or long-period comets; LPCs) and short-period Halley-type comets (HTCs). The precise distinction is arbitrary, based on a 200-year period that better reflects how long comets have been studied than anything else, but it is notable that the HTCs have somewhat flatter and more prograde inclinations than the nearly isotropic comets as a whole (Levison et al., 2001).

##### HTCs

The 22 currently known active HTCs pass  $q < 1.3$  AU at a rate of 0.46 per annum. Levison et al. (2002) argue based on their numerical simulations that HTCs have a uniform perihelion distribution, i.e., that  $N(<q) \propto q$ . Although the discovery rate is very low, Levison et al. (2002) argue that the current roster of nearby HTCs is only about 26% complete. With these augmentations the current flux of HTCs through the Solar System would be

$$\dot{N}(<q) = 1.8 \left( \frac{q}{1.3 \text{ AU}} \right). \quad (20)$$

HTCs are a dynamically evolved population that is well known to be depleted in small comets (Hughes, 1988). Levison et al. (2002) adopt  $N(>d) \propto d^{-1.4}$ , which is consistent with the consensus of opinion. The average collision rate of Jupiter with comets in parabolic orbits with isotropic inclinations with  $q \leq 5.2$  AU for a uniform perihelion distribution is  $1.0 \times 10^{-7}$  per comet per perihelion passage. If we use this impact rate to approximate that by HTCs, and if we take  $d = 3$  km as the size cutoff for the observed population, we obtain a current impact rate of active HTCs on Jupiter of

$$\begin{aligned} \dot{N}_J(d > 1.5) &= 7 \times 10^{-7} (1.5/3.0)^{-1.4} \\ &= 1.8 \times 10^{-6} \text{ per annum} \end{aligned} \quad (21)$$

with  $d > 1.5$  km. This is a small impact rate compared to that of JFCs, although the impact rates are less unequal for

distant satellites where the gravitational focusing by the central planet is relatively unimportant (see Eq. (3)).

Dormant HTCs are probably more important. Levison et al. (2002) report that there are nine known inactive HTCs, all with  $q < 2.5$  AU, with a median  $H = 14$ . This value of  $H$  corresponds to  $d = 12$  km for an albedo of 0.04. Levison et al. (2002) correct for the survey's discovery statistics given  $N(<q) \propto q$  and  $N(<d) \propto d^{-1.4}$ , and they extrapolate to  $d = 1.7$  km (i.e.,  $H = 18$ ) using  $b = 1.4$ . They estimate that 18 dormant HTCs pass perihelion with  $d > 1.7$  km with  $q < 3$  AU per annum. If we extrapolate the population out to Jupiter and use the same impact rate per comet for HTCs that we used previously,  $1.0 \times 10^{-7}$  per perihelion passage, we obtain for the dormant HTCs

$$\begin{aligned} \dot{N}_J(d > 1.5) &= 18 \times 10^{-7} (1.5/1.7)^{-1.4} \\ &= 3.7 \times 10^{-6} \text{ per annum} \end{aligned} \quad (22)$$

with  $d > 1.5$  km. Using  $N(<q) \propto q$  and parabolic orbits, the relative impact rates on Saturn, Uranus, and Neptune to that on Jupiter are 0.27, 0.018, and 0.019.

The power law  $N(>d) \propto d^{-1.4}$  is unlikely to hold for larger comets. Here we arbitrarily steepen the slope to  $b = 2.5$  for  $d > 20$  km. This is the same slope that we use for larger LPCs.

##### LPCs

Weigert and Tremaine (1999) estimate that  $\sim 36$  active LPCs pass within 3 AU of the Sun each year. LPCs do not appear to follow the uniform  $N(<q) \propto q$  perihelion distribution. Apparently interactions with the Sun and planets produce a relative deficit of LPCs near the Sun. For example, Everhart (1967) suggested that  $N(<q) \propto 0.4q + 0.3q^2$  and Kresak and Pittich (1978) suggested that  $N(<q) \propto q^{1.5}$ ; the two distributions are essentially the same for  $q < 3$  AU for which they apply. Weissman (1989) and L. Dones (personal communication) have found still steeper distributions in numerical simulations of Oort cloud genesis and evolution;  $N(<q) \propto q^2$  seems a fair approximation to their work:

$$\dot{N}(<q) = 36(q/3 \text{ AU})^2 \text{ per annum.} \quad (23)$$

The different mix of orbits produces a slightly higher average impact rate on Jupiter of  $1.5 \times 10^{-7}$  per annum for parabolic comets. The impact rate on Jupiter would be

$$\dot{N}_J(<q) = 1.6 \times 10^{-5} \text{ per annum.} \quad (24)$$

Impact rates for the more distant planets are obtained using  $N(<q) \propto q^2$ . This gives the largest number of comets and so maximizes the impact rate. For LPCs in parabolic orbits the relative impact rates on Saturn, Uranus, and Neptune to that on Jupiter are 0.50, 0.07, and 0.11.

As with other comet populations, how the number of LPCs scales with comet size is debatable. For fainter comets the distribution of active magnitudes is consistent with a power law  $N(>d) \propto d^{-2}$ . Everhart (1967) and Weissman (1991; see also Weissman and Levison, 1997) have argued that for  $d > 10$  km the power law is much steeper,  $N(>d) \propto d^{-3.5}$ . This is reminiscent of what we previously claimed for JFCs and ecliptic comets, although we restricted the steep slope to larger comets, Centaurs, and Kuiper Belt objects with  $d > 30$  km. In our opinion a distribution this steep for  $d < 30$  km makes comets like Hale–Bopp too rare; Hale–Bopp and comets like it (e.g., 1811) are better fit by a distribution no steeper than the classic collisional cascade  $N(>d) \propto d^{-2.5}$  (ZDL98). If we take  $d = 1.5$  km as corresponding to the magnitude cutoff for active LPCs, we obtain

$$\dot{N}_J(>d) = \begin{cases} 5.6 \times 10^{-7} (d/8)^{-2.5} & (d > 8 \text{ km}) \\ 1.6 \times 10^{-5} (d/1.5)^{-2.0} & (d < 8 \text{ km}) \end{cases} \quad (25)$$

We use Eq. (25) to describe the rate that active LPCs hit Jupiter.

There are only two known dormant LPCs. If the same perihelion and size distributions applied to dormant LPCs as to active HTC, dormant LPCs would be about 20% as important as dormant HTCs. But the size and space distributions could be different, and the observed dormant comets are quite large ( $d \approx 12$  km). What Levison et al. (2002) effectively report, when extrapolated back to the size of things that are actually observed, is that  $\sim 0.26$  dormant LPCs with  $d > 12$  km pass  $q < 3$  AU per annum. If we take the size distribution in Eq. (25) and the space distribution in Eq. (23), the resulting impact rate at Jupiter becomes for dormant LPCs

$$\dot{N}_J(>d) = \begin{cases} 3.2 \times 10^{-7} (d/8)^{-2.5} & (d > 8 \text{ km}) \\ 9.2 \times 10^{-6} (d/1.5)^{-2.0} & (d < 8 \text{ km}) \end{cases} \quad (26)$$

This is nearly three times higher than the impact rate by dormant HTCs, and not much smaller than the impact rate by active LPCs.

When all the NICs are summed together, they generate an impact rate on Jupiter for  $d = 1.5$  km that is about 1% that by JFCs (Fig. 2). Because the NICs are much less gravitationally concentrated than the ecliptic comets, they can be relatively less unimportant for the outlying satellites. In particular, the NICs could be an important source of small craters on Iapetus, Pluto, and Charon if the ecliptic comets are depleted in small comets and the LPCs are not.

We scale them through the outer Solar System according to the perihelia distributions already discussed, uniform for the HTCs and  $n(<q) \propto q^2$  for the LPCs, and use Eq. (3) to determine the impact rates on satellites vs those on the planets.

#### 4.7. Trojan asteroids

Shoemaker et al. (1989) estimated that there are  $\sim 2000$  Trojan asteroids bigger than  $d > 17$  km (for an assumed albedo of 0.04). We assume that the Trojan L4 and L5 clouds are substantially the same. According to Shoemaker et al. (1989) the smaller objects follow a  $N(>d) \propto d^{-2.17}$  power law. This is an extrapolation from the  $\sim 50$  Trojans with  $d > 100$  km for which observations were reasonably complete. The extrapolation makes use of independent re-discoveries of asteroids to estimate the incompleteness of the surveys. The largest objects, for which the survey is reasonably complete, follow a different and much steeper power law,  $N(>d) \propto d^{-3.75}$ . It is a bit disconcerting that the slope should change so drastically precisely where the survey's completeness also changes. In any event, when extrapolated to small objects, Shoemaker et al.'s estimate is equivalent to 390,000 Trojans with  $d > 1.5$  km.

In a more recent survey Jewitt et al. (2000) obtain a more direct estimate of the number of small Trojans in the L4 cloud. They estimate that there are 160,000 trojans librating around L4 with diameters  $d > 2$  km, in obeisance to the power law  $N(>d) \propto d^{-2 \pm 0.3}$ . This estimate extrapolates to 570,000 Trojans with  $d > 1.5$  km.

Levison et al. (1997) simulated orbital evolution of Trojan asteroids. They found that the dynamical lifetime of the average Trojan asteroid is 35 byr. LD97 elsewhere showed that  $\sim 2\%$  of JFC-like test particles hit Jupiter. If we presume that the same fraction applies to escaped Trojans, and we combine this with Jewitt et al.'s numbers and Shoemaker et al.'s size distributions, we obtain annual impact rates on Jupiter of

$$\dot{N}(>d) = \begin{cases} 4.4 \times 10^{-11} (d/100)^{-3.75} & (d > 100 \text{ km}) \\ 4.4 \times 10^{-11} (d/100)^{-2.17} & (d < 100 \text{ km}) \end{cases} \quad (27)$$

For  $d = 1.5$  km the impact rate is  $4 \times 10^{-7}$  per annum. This is about four orders of magnitude smaller than the corresponding JFC impact rate. This rate—which is based on the original sources and so omits errors that appeared in between—is much smaller than what we estimated incorrectly in ZDL98.

To raise this rate appreciably requires that collisions dominate ejection. Collisional ejection has been proposed (Marzari et al., 1998). However, it is likely to be mass dependent. In particular, small objects are more likely to be collisionally ejected. Here the absence of small craters on Europa, on Gilgamesh, and on Callisto in general and on Lofn in particular makes an argument against the Trojans

Table 3

Cratering rates (uncertain to a factor of 3) at Jupiter, assuming an impact rate on Jupiter of 0.005 comets per annum with  $d > 1.5$  km

	Cratering rates					Cratering time scale $\tau_A(>20)^f$	Disruption time scale $\tau_A(>2R_s)^g$
	$\dot{C}_A(>1)^a$	$\dot{C}_A(>10)^b$	$\dot{C}_A(>30)^c$	$\dot{C}_{NIC}(>10)^d$	$\dot{C}_S(>10)^e$		
Metis	$1.1 \times 10^{-11}$	$5.9 \times 10^{-13}$	$1.6 \times 10^{-13}$	$2.2 \times 10^{-14}$		130	0.8
Amalthea	$6.6 \times 10^{-12}$	$3.5 \times 10^{-13}$	$9.5 \times 10^{-14}$	$1.1 \times 10^{-14}$		60	1.6
Thebe	$7.8 \times 10^{-12}$	$4.1 \times 10^{-13}$	$1.1 \times 10^{-13}$	$1.9 \times 10^{-14}$		1100	2.4
Io	$5.1 \times 10^{-13}$	$2.7 \times 10^{-14}$	$4.1 \times 10^{-15}$	$3.6 \times 10^{-16}$	$5.2 \times 10^{-14}$	2.7	
Europa	$5.0 \times 10^{-13}$	$3.2 \times 10^{-14}$	$8.5 \times 10^{-15}$	$1.1 \times 10^{-15}$	$4.5 \times 10^{-14}$	2.2	
Ganymede	$2.7 \times 10^{-13}$	$1.8 \times 10^{-14}$	$4.2 \times 10^{-15}$	$7.2 \times 10^{-16}$	$2.3 \times 10^{-14}$	1.4	
Callisto	$1.5 \times 10^{-13}$	$9.8 \times 10^{-15}$	$2.1 \times 10^{-15}$	$6.0 \times 10^{-16}$	$1.2 \times 10^{-14}$	3.1	
Himalia	$2.4 \times 10^{-14}$	$1.3 \times 10^{-15}$	$2.2 \times 10^{-16}$	$5.5 \times 10^{-16}$		21,000	

<sup>a</sup> Case A cratering rate,  $D > 1$  km per  $[\text{km}^{-2} \text{ year}^{-1}]$ .  
<sup>b</sup> Case A cratering rate,  $D > 10$  km  $[\text{km}^{-2} \text{ year}^{-1}]$ .  
<sup>c</sup> Case A cratering rate,  $D > 30$  km  $[\text{km}^{-2} \text{ year}^{-1}]$ .  
<sup>d</sup> HTC and LPC (= NIC) cratering rate,  $D > 10$  km  $[\text{km}^{-2} \text{ year}^{-1}]$ .  
<sup>e</sup> Shoemaker and Wolfe’s cratering rates,  $D > 10$  km  $[\text{km}^{-2} \text{ year}^{-1}]$ .  
<sup>f</sup> Case A time scale for  $D > 20$  km craters [Myr].  
<sup>g</sup> Case A catastrophic disruption time scale [Gyr].

being an important cratering population at the  $d \approx 100$  m scale; for if they were important, they would be collisional, and the distribution of crater sizes would be steep. At still smaller scales (meteors  $< 10$  m), where comets are few and where Europa at least has many pits, it is imaginable that Trojans contribute or dominate. If little Trojans do dominate at the pitting scale, collisional ejection would need to be  $\sim 100$  times more efficient than dynamical ejection for  $< 10$ -m objects. This does not seem impossible.

**5. Results**

In this section we will quote characteristic time scales at the current impact rate, but when we give specific ages for cratered surfaces we will assume that the impact flux declines as  $t^{-1}$  (Holman and Wisdom, 1993).

*5.1. Jupiter*

Cratering rates on the Galilean satellites are substantially revised from what we quoted in 1998. For 10-km craters these are typically about 70% of those recommended by Shoemaker (Shoemaker and Wolfe, 1982). But for 30-km craters our rates are about twice as great as Shoemaker and Wolfe’s. Differences are mostly attributable to different size–number distributions of comets. Recommended cratering rates at Jupiter are summarized in Table 3 and Fig. 3.

*Metis, Thebe, and Amalthea*

These moons all have time scales against collisional disruption that are on the order of a billion years. We will discuss the issue of collisional disruption more generally later. Here we note that it is unlikely that any have survived 4 Gyr unscathed in their present form in their present orbits.

*Europa*

Europa’s surface is considerably older than the 10 Myr estimated by ZDL98. The average crater density of the well-mapped swaths is  $C(\geq 1) \approx 30$  per  $10^6 \text{ km}^2$  (Schenk et al., 2003). The corresponding nominal surface age is 60 Myr. An alternative approach is to use larger craters. The best current estimate for the number of 20-km craters on Europa is about 12 to 30. At an average rate of one 20-km crater per 2.2 Myr (Table 3), we choose an average age of Europa’s surface between 30 and 70 Myr.

In these estimates we have excluded obvious secondaries from the count of kilometer-size craters, but we have not been aggressive about this. We cannot exclude planetocentric cratering caused by ejecta launched into joventric orbit—these craters would not cluster or line up along crater

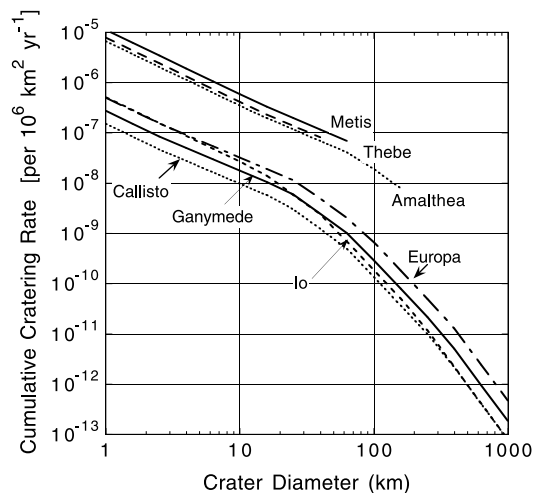


Fig. 3. Cumulative cratering rates at Jupiter. The curves for Metis, Thebe, and Amalthea are truncated for craters larger than the satellite. Such impacts are deemed disruptive.

rays as secondaries do. Such belated secondaries would be indistinguishable from primary craters. If present, they would imply an even younger surface for Europa. However, classical secondary craters are known to have a steep size–frequency distribution akin to a collisional population (e.g., Melosh, 1989). There is every reason to expect the same of planetocentric debris (e.g., Croft et al., 1995). The remarkably shallow slope of the 1- to 10-km-diameter european craters would seem to exclude significant numbers of secondaries of any type. Moreover, the largest ordinary secondaries are typically only about 3–4% the diameter of the primary crater (Melosh, 1989, p. 101); therefore on Europa the largest secondaries are likely to be <2 km across. In a discussion of the ganymedean Gilgamesh impact, Alvarellos et al. (2002) found that about 70% of the ejecta from Ganymede that escaped into orbit about Jupiter eventually hit Ganymede; about 12% hit Callisto and another 10% hit Europa. The rest hit Io, escaped into heliocentric space, or hit Jupiter. By scaling from large lunar and vestan craters to Gilgamesh, Alvarellos et al. (2002) estimated that the largest blocks launched at escape velocity would have been on the order of 1 km, typically making ~4-km craters on Ganymede. Scaling by the size of the primary craters implies that we do not expect planetocentric secondaries to be important on Europa at sizes larger than about 300 m. (It is possible but by definition unlikely that a much larger crater than any on Europa formed on Ganymede during the same interval of time sampled by Europa’s surface. If so, then ejecta from Ganymede would be important to Europa, and planetocentric secondaries larger than 300 m would form.) Material properties do play a part in choosing this size, a factor that Alvarellos et al. (2002) neglected in making their estimate. Presumably a stronger, more coherent target would make for bigger secondaries.

### *Ganymede*

The average crater density on the bright terrains corresponds to an average age of 2 Gyr. It has been 1 Gyr since nonsynchronous rotation stopped. These ages are very uncertain; they also have a small element of circular reasoning in them, since we assumed that  $T_{BD} = 1$  Gyr to set one of the constraints on the jovian cratering rate.

The age of Gilgamesh is perhaps more interesting. Crater densities on the ejecta blanket, although low, are much higher than the crater densities on Europa. Assume that Gilgamesh postdates synchronicity. The local cratering rate at  $\beta = 65^\circ$  is about 45% higher than the global average. At a crater density of  $C(>22 \text{ km}) = 22 \text{ per } 10^6 \text{ km}^2$ , the age would be 800 Myr.

### *Callisto*

Callisto is mostly old. However, the basins Lofn and Valhalla appear to be younger. Both Lofn and Valhalla are assigned nominal ages of 2 Gyr, although Valhalla is twice as densely cratered. Because Valhalla is not far from the apex of motion, cratering rates there are high. The higher

crater densities on Valhalla make its relative age much less secure—there could be saturation effects.

### *Himalia*

Himalia is included as a proxy for the irregular outer satellites. Cratering rates by comets are exceedingly low. At current rates, Himalia averages fewer than one 10-km crater per age of the Solar System. By contrast, impact probabilities with the other irregular satellites are much higher. Nesvorný et al. (2003) find that Himalia is struck by another member of its group on time scales comparable to the age of the Solar System. The implication is that the irregular satellite systems are evolving nicely on their own, without much help from comets.

### 5.2. *Saturn*

Small craters are abundant near Saturn. What is unclear is whether the impactors were comets from outside the system, or whether they were planetocentric debris issuing from some cataclysm (Smith et al., 1981, 1982; Chapman and McKinnon, 1986; Lissauer et al., 1988). The two choices are named population I and population II, respectively. In this picture population I is (or was) responsible for the larger craters, while population II is responsible for most of the small craters. Population II is relatively rich in small bodies and deficient in large ones, which would be consistent with a catastrophic collisional origin. The reality of the two populations has been questioned by Lissauer et al. (1988), who argued instead that there is but one population, population I, a heliocentric population that is rich in small bodies but not deficient in large ones. They would account for the apparent existence of two populations through the effects of crater saturation.

We begin with the assumption that the impactors are heliocentric. For Saturn and beyond we will consider two cases. In Case A, the mass distribution of small comets is consistent with what we find at Jupiter. This requires the two population model to produce crater size–frequency distributions that are sufficiently steep at small sizes. In Case B, we use a mass distribution of small comets that can account for the larger number of small craters on Triton. The latter permits models consistent with the position taken by Lissauer et al. (1988). We note that the relative dearth of small heliocentric comets at Jupiter requires substantial evolution of the size–frequency distribution of comets in Case B as they migrate inward. For the small moons of Saturn, where small comets make big craters, the two cratering rates are quite different (see Table 4).

Previous estimates of cratering rates at Saturn were made by Smith et al. (1982) and Lissauer et al. (1988). Smith et al. estimate absolute cratering rates for 10-km craters. A direct comparison is possible. We find that our cratering rates at Saturn are generally much higher than estimated by Smith et al. (1982), save for the outermost satellites. Even our Case A estimates, which are low because Case A assumes few

Table 4

Cratering rates (uncertain to a factor of 4) at Saturn, assuming an impact rate on Saturn of 0.002 comets per annum with  $d > 1.5$  km

	Cratering rates				Cratering times		Disruption times		
	$\dot{C}_A(>10)^a$	$\dot{C}_B(>10)^b$	$\dot{C}_S(>10)^c$	$\dot{C}_{NIC}(>10)^d$	$\tau_A(>20)^e$	$\tau_B(>20)^f$	$\tau_A^g$	$\tau_B^h$	$\tau_S^i$
Ring moon <sup>j</sup>							11	11	32
Prometheus	$3.5 \times 10^{-13}$	$5.6 \times 10^{-12}$	$3.2 \times 10^{-14}$	$3.7 \times 10^{-15}$	210	23	1.4	0.6	120
Pandora	$3.0 \times 10^{-13}$	$5.0 \times 10^{-12}$	$3.2 \times 10^{-14}$	$3.8 \times 10^{-15}$	340	37	1.8	0.6	130
Epimetheus	$2.5 \times 10^{-13}$	$3.8 \times 10^{-12}$	$2.4 \times 10^{-14}$	$2.9 \times 10^{-15}$	210	25	2.0	1.0	190
Janus	$2.2 \times 10^{-13}$	$3.1 \times 10^{-12}$	$2.4 \times 10^{-14}$	$2.6 \times 10^{-15}$	95	12	2.4	2.0	200
Mimas	$9.9 \times 10^{-14}$	$8.8 \times 10^{-13}$	$1.6 \times 10^{-14}$	$1.0 \times 10^{-15}$	50	9.7	21	21	360
Enceladus	$7.0 \times 10^{-14}$	$5.7 \times 10^{-13}$	$1.0 \times 10^{-14}$	$8.0 \times 10^{-16}$	42	9.4	45	45	360
Tethys	$4.4 \times 10^{-14}$	$2.9 \times 10^{-13}$	$4.3 \times 10^{-15}$	$5.5 \times 10^{-16}$	15	4.1	400	400	1200
Telesto	$1.4 \times 10^{-13}$	$2.1 \times 10^{-12}$	$8.4 \times 10^{-15}$	$1.8 \times 10^{-15}$	11,000	1300	12	1.6	250
Calypso	$1.4 \times 10^{-13}$	$2.1 \times 10^{-12}$	$8.4 \times 10^{-15}$	$1.8 \times 10^{-15}$	11,000	1300	12	1.6	250
Dione	$3.0 \times 10^{-14}$	$1.9 \times 10^{-13}$	$2.7 \times 10^{-15}$	$4.2 \times 10^{-16}$	20	5.7	840	840	2100
Helene	$9.3 \times 10^{-14}$	$1.2 \times 10^{-12}$	$6.1 \times 10^{-15}$	$1.4 \times 10^{-15}$	8000	1000	13	2.6	490
Rhea	$1.9 \times 10^{-14}$	$1.0 \times 10^{-13}$	$1.5 \times 10^{-15}$	$3.2 \times 10^{-16}$	17	5.5	3100	3100	3800
Titan	$6.0 \times 10^{-15}$	$2.4 \times 10^{-14}$	$1.3 \times 10^{-15}$	$1.8 \times 10^{-16}$	(5.0)	(2.2)			5500
Hyperion	$9.0 \times 10^{-14}$	$5.8 \times 10^{-14}$	$1.8 \times 10^{-15}$	$4.3 \times 10^{-16}$	1300	350	330	330	2000
Iapetus	$1.9 \times 10^{-15}$	$7.4 \times 10^{-15}$	$7.9 \times 10^{-16}$	$2.2 \times 10^{-16}$	230	110			6400
Phoebe	$6.0 \times 10^{-16}$	$2.7 \times 10^{-15}$	$1.3 \times 10^{-15}$	$2.2 \times 10^{-16}$	27,000	11,000			2300

<sup>a</sup> Case A cratering rate,  $D > 10$  km [ $\text{km}^{-2} \text{year}^{-1}$ ].  
<sup>b</sup> Case B cratering rate,  $D > 10$  km [ $\text{km}^{-2} \text{year}^{-1}$ ].  
<sup>c</sup> Smith et al. (1982) cratering rates,  $D > 10$  km [ $\text{km}^{-2} \text{year}^{-1}$ ].  
<sup>d</sup> HTC and LPC (= NIC) cratering rate,  $D > 10$  km [ $\text{km}^{-2} \text{year}^{-1}$ ].  
<sup>e</sup> Case A time scale for  $D > 20$  km craters [Myr].  
<sup>f</sup> Case B time scale for  $D > 20$  km craters [Myr].  
<sup>g</sup> Case A catastrophic disruption time scale [Gyr].  
<sup>h</sup> Case B catastrophic disruption time scale [Gyr].  
<sup>i</sup> Smith et al. (1982) catastrophic disruption time scale [Gyr].  
<sup>j</sup> A moon the size of Mimas placed at the Roche limit (here 2.17 Rs), in what is now the A ring.

small comets, are typically a factor of 10 higher for 10-km craters. For Rhea inward, the Case B estimates are closer to 100 times higher for 10- to 30-km craters. These are large differences. On the other hand, apart from Iapetus and Phoebe, we obtain about the same pattern of relative cratering rates between satellites. Our cratering rates in the Saturn system are illustrated in Figs. 4–6. Nominal surface ages based on archival crater counts for the Saturn system are illustrated in Fig. 7. These ages are upper limits because we have neglected planetocentric cratering.

Lissauer et al. (1988) address only the relative cratering rates. They assume a very high 10 km/s average encounter velocity of comets with Saturn, and so they find much less gravitational focusing and a much flatter distribution of cratering rates through the system. The high encounter speed with Saturn is almost certainly wrong (cf. LD97).

Mimas appears heavily cratered to the point of saturation with small craters, but it has relatively few craters bigger than 30 km in diameter. There is no obvious sign of an apex–antapex cratering asymmetry. Given the observed density of 10-km craters and the (low) Case A heliocentric cratering rates, the surface would seem to be ancient, at least 4-Gyr old. But the low abundance of large craters suggests a young surface. According to crater counts by Lissauer et al. (1988), the density of  $D > 32$  km craters (1-km comets)

is about 40 per  $10^6 \text{ km}^2$ . This low density suggests a surface age of 1.3 Gyr in Case A and 0.4 Gyr in Case B.

The young ages are probably the better estimates, as there are other sources of small impactors. One good reason is the presence, in the 130-km crater Herschel, of a plausible source of large blocks of ejecta. To estimate the number of

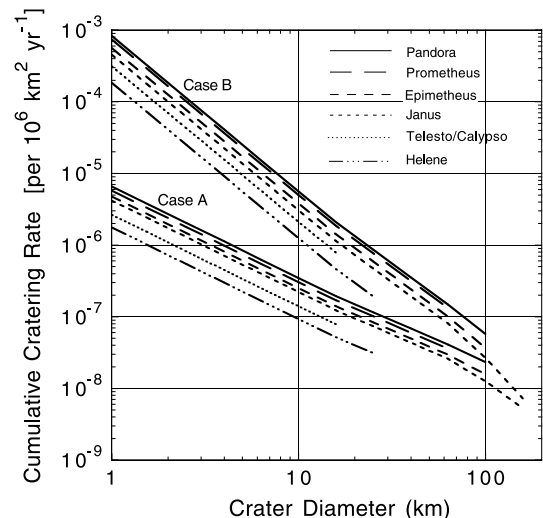


Fig. 4. Cumulative cratering rates for the Voyager inner moons of Saturn. Both Cases A and B are shown.

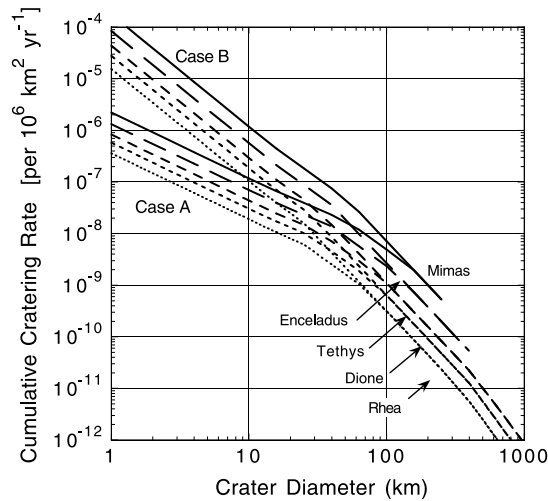


Fig. 5. Cumulative cratering rates for the classical inner moons of Saturn. Both Cases A and B are shown.

large blocks likely to have been ejected into orbit about Saturn during the excavation of this crater, we draw an analogy to the asteroid Vesta. At least twenty 5- to 10-km-size blocks were launched into heliocentric space in the process of excavating a 460-km crater on Vesta, along with at least another 200 smaller vestoids (Drake, 2001; Burbine et al., 2001). To first approximation we will assume that the largest block size is linearly proportional to the size of the crater. Melosh (1989, p. 105) also points out that the largest block size is inversely proportional to the ejection velocity. Hence we estimate that the largest ejected block scales as  $D/v_{esc}$ . The escape velocity from Vesta is 360 m/s and the escape velocity from Mimas is 160 m/s. Hence we estimate that Herschel launched at least twenty 3 to 6-km blocks and a larger number of smaller ones. At 1.5 km/s, a reasonable velocity for impacts on Mimas by objects in planetocentric orbit at Mimas, the typical 4-km ejectum produces a 30-km

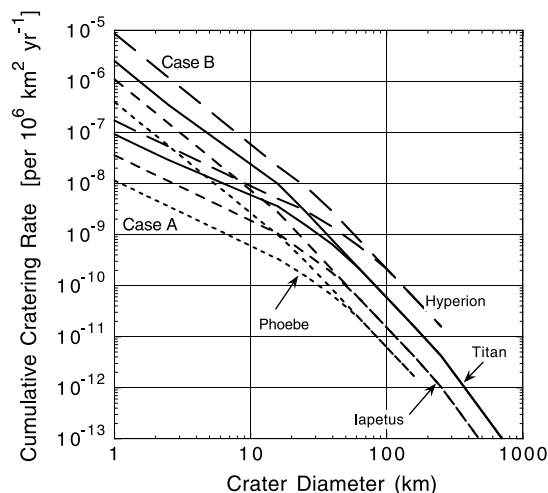


Fig. 6. Cumulative cratering rates for the classical outer moons of Saturn. Both Cases A and B are shown.

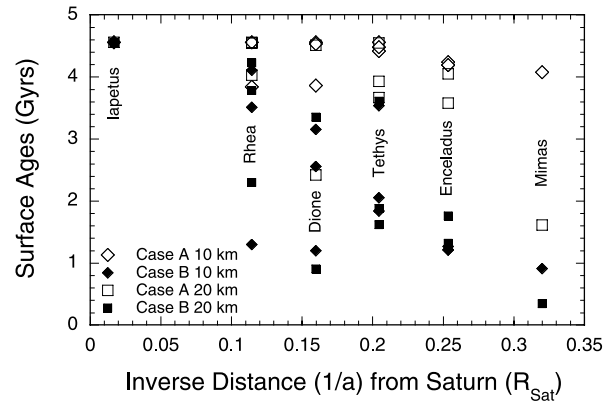


Fig. 7. Some illustrative surface ages in the saturnian system. These use Voyager era crater counts and take into account the apex angle  $\beta$  where relevant. Note that Enceladus's surface need not be especially young. Indeed, by Case A, Enceladus could be very old. This occurs because the sparsely cratered terrains of Enceladus are at high apex angle  $\beta$ . Note also that heavily cratered Mimas need not be exceptionally old. Indeed, there seems to be no particular reason to think that the young terrains of any of the moons interior to Titan are any older or younger than those of the others.

crater. Given a steep size distribution  $b \approx 2.5$  appropriate to ejecta, we estimate that Herschel produced 30–100 craters on Mimas with  $D > 20$  km. The actual number of craters with  $D > 20$  km on Mimas is  $\sim 70$ . Thus, to first approximation, most of the craters on Mimas smaller than 30 km could be planetocentric, with their origin in the Herschel cratering event (itself the product of the impact of a 4-km ecliptic comet). Mimas may tell us nothing about the population of small heliocentric comets in the Saturn system.

Enceladus features some apparently lightly cratered terrains on its trailing hemisphere. Although crater densities on Enceladus appear to involve some geological control, it is also true that the low crater densities are antipical. If Enceladus has stayed in synchronous lock its surface need not be especially young. Even given the higher impact fluxes of Case B, ages could be as high as 1 Gyr. In particular, apart from its remarkable whiteness, there is no evidence that the surface of Enceladus is any younger than the surface of Mimas. The whiteness is presumably related to the E Ring, and both are most easily understood as the result of a fairly recent impact on Enceladus. The lifetime of the E Ring therefore holds promise as an independent chronometer. However, it has been suggested that the E Ring is a semi-permanent feature (Hamilton and Burns, 1994). If so, it would be useless as a chronometer.

Surfaces on Tethys, Dione, and Rhea seem to range from 1 to 4 Gyr depending on assumptions. On all three, planetocentric cratering might be important. Cratering of Iapetus is very slow and its surface would appear to be extremely old. Discussion of Titan will be deferred to a later paper in which the atmosphere will play a major part.

It has been suggested that a satellite breaks up if the expected crater diameter exceeds the satellite's diameter (e.g., Smith et al., 1981, 1982). In any case such craters are

Table 5  
Disruptions at Saturn

Moon	Smith et al. Iapetus <sup>b</sup>	Lissauer et al.		Case A		Case B	
		Rhea <sup>a</sup>	Iapetus <sup>b</sup>	Rhea <sup>a</sup>	Iapetus <sup>b</sup>	Rhea <sup>a</sup>	Iapetus <sup>b</sup>
Ring moon	12	0.27–0.56	0.9–3.9	0.18	2.9	0.08	2.0
Prometheus	12	0.8–1.45	2.4–9.8	1.4	23	1.6	38
Pandora	13	1.0–1.9	3.1–12.6	1.1	18	1.5	36
Epimetheus	9			1.0	16	0.91	21
Janus	8	0.4–0.75	1.3–5.2	0.82	13	0.45	11
Mimas	4.7	0.16–0.26	0.51–1.85	0.092	1.5	0.043	1.0
Enceladus	4.3	0.09–0.13	0.29–0.95	0.043	0.7	0.020	0.47
Tethys	1.1	0.03–0.04	0.11–0.31	0.005	0.08	0.002	0.05
Telesto	4	2.3–3.2	7–20	0.16	2.6	0.58	14
Calypso	4	2.3–3.2	7–20	0.16	2.6	0.58	14
Dione	0.66	0.02–0.03	0.08–0.2	0.002	0.04	0.001	0.03
Helene	3			0.15	2.4	0.35	8.3
Rhea	0.29	0.01	0.04–0.09	0.001	0.01		0.007
Titan	0.24						
Hyperion	0.59	0.03–0.05	0.16–0.22	0.006	0.10	0.003	0.066
Iapetus	0.18	0.003–0.007	0.02				
Phoebe	0.63	0.02–0.07	0.17–0.21		0.003		0.002

<sup>a</sup> Number of disruptions implied by the craters on Rhea.

<sup>b</sup> Number of disruptions implied by the craters on Iapetus.

not and perhaps cannot be seen; at a minimum the surface is reborn. We shall call such an impact “disruptive.” Table 5 lists disruption time scales at Saturn at current impact rates. Modern low densities of inner moons are used (Yoder et al., 1989; Nicholson et al., 1992; McGhee et al., 2001). We expect that a 400-km crater on Mimas requires an 18-km-diameter impactor releasing about  $10^{31}$  ergs, which exceeds the gravitational binding energy of Mimas ( $0.6GM^2/R$ ) by a factor of 5. (The same energy could be dispersed by raising the temperature of Mimas by a mere 10 K, which implies that disruption is not the only option.) At current impact rates Mimas experiences such events on a  $\tau_B \approx 20$  Gyr time scale. This is already a rather high rate, implying a 17% chance of disruption over 4 Gyr even if impact rates had remained constant. If we make the more aggressive assumption that the Kuiper Belt disperses as  $t^{-1}$  from an origin at 4.56 Gyr the ago, the chance that Mimas was collisionally disrupted in the past 4 Gyr is about 36%.

The inner small saturnian satellites fare less well. The largest and most durable of these is 180-km-diameter Janus. At current impact rates Janus would be disrupted by a 4-km comet on a 2.2-Gyr time scale; Janus has an 80% chance of being collisionally disrupted in 4 Gyr at current impact rates. If the  $t^{-1}$  flux history applies, Janus has a 99% chance of being disrupted in the past 4 Gyr. The smaller inner satellites are disrupted more easily still, although the details depend on whether one chooses Case A or Case B. The low densities of these moons offer circumstantial evidence for a rubble pile interpretation of these bodies.

It is interesting to ask how long a Mimas-sized satellite would last at the distance of the rings. Such a body if shattered could give rise to a system of rings like Saturn’s; at least the mass might be adequate. The nominal answer at

the distance of the A ring ( $2.17 R_s$ , the nominal location of the Roche limit for an assumed density of  $0.9 \text{ g/cm}^3$ ) is about  $\sim 11$  Gyr, with the breakup probability over 4 Gyr being 60% if the flux declined as  $t^{-1}$ . The cause would be a  $\sim 15$ -km-diameter comet. These are perhaps reasonable probabilities for an event that is unlikely to be commonplace. On the other hand, as has been noted (Lissauer et al., 1988), it is undeniably improbable that such a moon could have escaped the heavy bombardment of the deep past only to be obliterated relatively recently.

Table 5 estimates the number of times a satellite has been disrupted while Rhea and Iapetus accumulated the craters they now have. This is how Smith et al. (1982) and Lissauer et al. (1988) presented their results. We use the same format to facilitate comparison. Both Rhea and Iapetus are heavily cratered. Because the cratering rate at Iapetus is much lower than at Rhea, its craters represent a longer period of bombardment. It is possible that NICs contributed significantly at Iapetus, although our best estimate is that they enter at the  $<10\%$  level (Table 5). Rhea and Iapetus can be viewed as bounds on the historical record. There do not appear to be any significant differences among the estimates for the space-age inner moons, save for the (putative) larger ring moon, where we agree with Lissauer et al. that the observable bombardment history of Saturn does not preclude the long-term survival of a large moon at the location of the rings. For the more substantial classical moons our disruption rates appear to be insignificantly lower than Lissauer et al.’s and much lower than Smith et al.’s.

It is also interesting to ask what the chances are of an SL9-like event occurring on Saturn during the active lifetime of the Cassini spacecraft. The likelihood of observing an SL9-like event depends strongly on whether one adopts

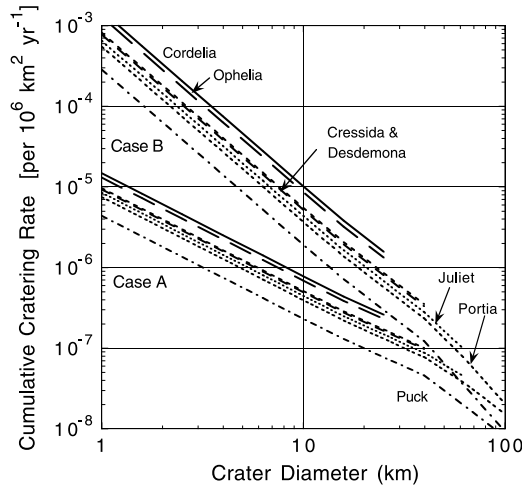


Fig. 8. Cumulative cratering rates for the Voyager inner moons of Uranus. Cases A and B are shown.

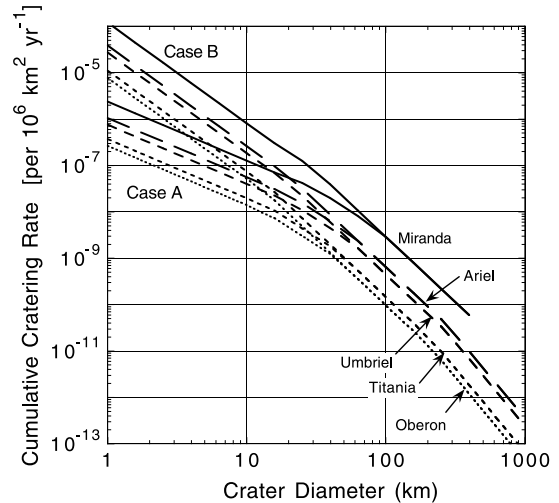


Fig. 9. Cumulative cratering rates for the classical moons of Uranus.

Case A or Case B at Saturn. Under Case B there is a 50% chance of a 270-m object striking Saturn during the 5 years or so that Cassini is active, and a 12% chance of a 600-m impact during the same interval. But under Case A, the 50% impactor would be only 30 m, and there is just a 2.5% chance of a 600-m impact.

### 5.3. Uranus

Our cratering rates at Uranus are higher than earlier estimates given by Smith et al. (1986), but the difference between new and old is not as great as it is at Saturn, nor is it as well founded, because the systematic uncertainties are also larger than at Saturn. For 10-km craters in Case A, the difference is a factor of 2 or less, rising to a factor of 4 for 30-km craters. For Case B the difference is about a factor of 10 or a little less. Cratering rates at Uranus are summarized in Figs. 8 and 9, and some nominal surface ages are shown in Fig. 10. Archival crater counts are from three studies by Plescia (1987a,b, 1989).

Miranda is the interesting object in the uranian system. It appears to be the sort of chimerical object we should be seeking. According to Eq (6), it takes a 36-km-diameter impactor to disrupt Miranda. We estimate that at current rates this happens about once every 45 Gyr. At constant flux the chance of a disrupting event in the past 4 Gyr is about 10%. If we use  $t^{-1}$ , the corresponding chance of disruption rises to about 20%. This is rather low for the archetype of disruption (Marzari et al., 1998). Perhaps we have underestimated the flux of large bodies through the uranian system or overestimated the size of disrupting impacts. But more likely, we need to count all the moons in the Solar System. If there are several moons each with a 10% chance of getting disrupted, there is a fair likelihood that one does.

Ariel may have regions as young as 1 or 2 Gyr although most of the crater counts imply ancient surfaces. However,

as has been discussed both in this paper and in many others, these ages become upper limits if planetocentric debris is important.

Of the classical moons, only Miranda and Ariel show any large areas that are obviously young. Miranda in particular appears to be, in places, fairly young. The youngest areas appear to be Inverness (the famous chevron-shaped feature) and Arden. In Case A both have nominal ages on the order of 1 Gyr. In Case B both have nominal ages on the order of 100 Myr. The third of the three coroneae, Elsinore, is much older, and would appear to be more or less the same age as most of the cratered terrain. In Case B this could be as young as 2 Gyr. The large gap in apparent ages between

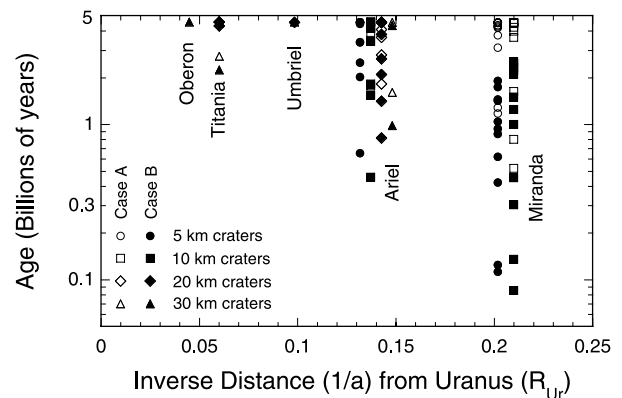


Fig. 10. Some illustrative surface ages in the uranian system. These use Voyager era crater counts and take into account the apex angle  $\beta$ . Miranda has surfaces that are clearly young, provided that the present orientation of Miranda has endured. Subject to this constraint, the two young provinces are Arden and Inverness. Arden is heavily cratered but, at  $\beta = 35^\circ$ , it would be young nonetheless. The third famous feature, Elsinore, is less heavily cratered than Arden but at  $\beta = 150^\circ$  is currently near the antapex where cratering rates are very low, and so it is nominally rated as very old. Ariel and Titania also may have relatively youthful provinces, while nothing young was seen on Umbriel or Oberon.

Table 6

Cratering rates (uncertain to a factor of 6) at Uranus, assuming an impact rate on Uranus of 0.00125 comets per annum with  $d > 1.5$  km

	Cratering rates				Cratering times		Disruption times		
	$\dot{C}_A(>10)^a$	$\dot{C}_B(>10)^b$	$\dot{C}_S(>10)^c$	$\dot{C}_{NIC}(>10)^d$	$\tau_A(>20)^e$	$\tau_B(>20)^f$	$\tau_A^g$	$\tau_B^h$	$\tau_C^i$
Cordelia	$7.8 \times 10^{-13}$	$1.0 \times 10^{-11}$		$1.5 \times 10^{-15}$	1400	190	1.9	0.3	0.3–0.9
Ophelia	$6.9 \times 10^{-13}$	$8.6 \times 10^{-12}$		$1.4 \times 10^{-15}$	1200	170	1.9	0.4	0.4–1.4
Bjanca	$5.4 \times 10^{-13}$	$6.2 \times 10^{-12}$		$1.1 \times 10^{-15}$	700	110	1.7	0.5	0.6–2.9
Cressida	$4.9 \times 10^{-13}$	$5.2 \times 10^{-12}$		$1.0 \times 10^{-15}$	390	67	1.5	0.7	0.9–6.2
Desdemona	$5.1 \times 10^{-13}$	$5.5 \times 10^{-12}$		$1.0 \times 10^{-15}$	500	83	1.5	0.6	0.8–5.0
Juliet	$4.4 \times 10^{-13}$	$4.4 \times 10^{-12}$		$8.9 \times 10^{-16}$	240	43	1.8	1.1	1.3–10
Portia	$3.9 \times 10^{-13}$	$3.7 \times 10^{-12}$		$8.1 \times 10^{-16}$	160	31	2.1	1.7	1.8–17
Rosalind	$4.6 \times 10^{-13}$	$4.9 \times 10^{-12}$		$9.3 \times 10^{-16}$	470	81	1.6	0.7	1.0–5.9
Belinda	$3.0 \times 10^{-13}$	$3.0 \times 10^{-12}$		$8.4 \times 10^{-16}$	530	95	2.6	1.3	1.3–9.1
Puck	$2.3 \times 10^{-13}$	$1.9 \times 10^{-12}$	$3.1 \times 10^{-13}$	$6.1 \times 10^{-16}$	130	29	4.9	4.9	4.0–56
Miranda	$1.3 \times 10^{-13}$	$8.1 \times 10^{-13}$	$1.1 \times 10^{-13}$	$3.8 \times 10^{-16}$	25	7.0	45	45	
Ariel	$5.6 \times 10^{-14}$	$2.6 \times 10^{-13}$	$4.3 \times 10^{-14}$	$2.1 \times 10^{-16}$	10	3.9			
Umbriel	$4.0 \times 10^{-14}$	$1.8 \times 10^{-13}$	$2.6 \times 10^{-14}$	$2.0 \times 10^{-16}$	13	5.3			
Titania	$2.0 \times 10^{-14}$	$7.4 \times 10^{-14}$	$1.1 \times 10^{-14}$	$1.5 \times 10^{-16}$	18	9			
Oberon	$1.4 \times 10^{-14}$	$5.2 \times 10^{-14}$	$7.9 \times 10^{-15}$	$1.4 \times 10^{-16}$	28	14			

<sup>a</sup> Case A cratering rate,  $D > 10$  km [ $\text{km}^{-2} \text{year}^{-1}$ ].<sup>b</sup> Case B cratering rate,  $D > 10$  km [ $\text{km}^{-2} \text{year}^{-1}$ ].<sup>c</sup> Smith et al. (1986) cratering rates,  $D > 10$  km [ $\text{km}^{-2} \text{year}^{-1}$ ].<sup>d</sup> HTC and LPC (=NIC) cratering rate,  $D > 10$  km [ $\text{km}^{-2} \text{year}^{-1}$ ].<sup>e</sup> Case A time scale for  $D > 20$  km craters [Myr].<sup>f</sup> Case B time scale for  $D > 20$  km craters [Myr].<sup>g</sup> Case A catastrophic disruption time scale [Gyr].<sup>h</sup> Case B catastrophic disruption time scale [Gyr].<sup>i</sup> Colwell et al. (2000) catastrophic disruption time scale [Gyr].

Elsinore and the cratered terrain, on the one hand, and Arden and Inverness, on the other, is a bit puzzling if one imagines that all of Miranda's oddities are tied to a single event.

Uranus has a large crop of small inner moons. They may not be old, in the sense that all of them, with the possible exception of Puck, are expected to be collisionally disrupted on time scales comparable to or shorter than the age of the Solar System; the likelihood that at least one has been disrupted in the geologically recent past is very high. Disruption time scales are listed in Table 6. Also listed for comparison are disruption times estimated by Colwell et al. (2000). Our Case B disruption times are essentially identical to the low end of Colwell's estimates: Owing to abundant small comets, most of the little moons last less than a billion years, and there is a wide scatter of lifetimes. The time scales would be much shorter still if we used Case C (the pure fragmentation distribution). But by the relaxed schedule of Case A all but Puck are expected to disrupt on the same  $\sim 2$ -Gyr time scale. (Puck endures for 5 Gyr.) It is interesting that they should all have similar life expectancies against external disruption. Collisional disruption rates are sensitive to satellite density. There is growing evidence that small bodies are generally underdense, so that our use of  $0.9 \text{ g/cm}^3$  is likely to be too great; a lower density would imply easier disruption, all other things being equal. One might expect that the disruption time scales of all these moons should be comparable to the age of the Solar System. This may be so; certainly we would not claim accuracy of better

than a factor of 2 (or 4 for that matter) at Uranus. One might also expect that the time scales should all be similar. To first approximation a disrupted moon should reaccrete in place, albeit into a smaller body than before as some ejecta would be lost to adjacent moons and maybe to other more distant sinks. The new smaller moon would be more easily disrupted. If a moon were to shrink enough that its collisional disruption rate became fast compared to its neighbors, it would quickly vanish to the enrichment of its neighbors. In this way the equal and long disruption time scales of Case A seem reasonable and appropriate, while the unequal and short disruptive time scales in Case B raise suspicions.

#### 5.4. Neptune system

The Neptune system poses the greatest problems. If we accept the LD97 impact rate on Neptune of 0.54 that of Jupiter, impact rates at Neptune are very high, in Case A roughly 5 times higher, and in Case B 40 times higher, than cratering rates estimated by Smith et al. (1989; for 10-km craters—Table 7). The high impact rates are due to the proximity of the Kuiper Belt. On the other hand it is important to recall that the limited range of initial conditions in the LD97 simulation are most troublesome at Neptune. In all likelihood the unrepresentatively low inclinations of the Kuiper Belt source in LD97 lead to a systematic overestimate of the relative impact rate on Neptune by a factor of 2 or more.

Table 7

Cratering rates (uncertain to a factor of 10) at Neptune and Pluto, assuming an impact rate on Neptune of 0.0013 comets per annum with  $d > 1.5$  km

	Cratering rates				Cratering times		Disruption times		
	$\dot{C}_A (>10)^a$	$\dot{C}_B (>10)^b$	$\dot{C}_S (>10)^c$	$\dot{C}_{NIC} (>10)^d$	$\tau_A (>20)^e$	$\tau_B (>20)^f$	$\tau_A^g$	$\tau_B^h$	$\tau_C^i$
Naiad	$7.9 \times 10^{-13}$	$9.3 \times 10^{-12}$	$5.0 \times 10^{-13}$	$2.1 \times 10^{-15}$	280	43	0.9	0.3	0.56–3.0
Thalassa	$7.3 \times 10^{-13}$	$8.0 \times 10^{-12}$	$4.1 \times 10^{-13}$	$1.8 \times 10^{-15}$	160	26	1.0	0.5	0.83–5.9
Despina	$5.7 \times 10^{-13}$	$5.4 \times 10^{-12}$	$2.1 \times 10^{-13}$	$1.4 \times 10^{-15}$	60	11	1.4	1.4	1.7–20
Galatea	$4.7 \times 10^{-13}$	$4.3 \times 10^{-12}$	$2.9 \times 10^{-13}$	$1.3 \times 10^{-15}$	63	12	2.0	2.0	2.3–29
Larissa	$3.7 \times 10^{-13}$	$3.2 \times 10^{-12}$	$1.6 \times 10^{-13}$	$1.0 \times 10^{-15}$	55	11	3.5	3.5	3.7–83
Proteus	$1.7 \times 10^{-13}$	$1.2 \times 10^{-12}$	$5.7 \times 10^{-14}$	$5.2 \times 10^{-16}$	25	6.6	23	23	25–12,000
Triton	$2.8 \times 10^{-14}$	$1.0 \times 10^{-13}$	$8.4 \times 10^{-15}$	$1.5 \times 10^{-16}$	4.2	2.0			
Nereid	$2.9 \times 10^{-15}$	$1.1 \times 10^{-14}$	$6 \times 10^{-16}$	$1.4 \times 10^{-16}$	2800	1400	6000	6000	
Pluto	$3.9 \times 10^{-14}$	$8.4 \times 10^{-14}$		$6.6 \times 10^{-17}$	5.6	4.9			
Charon	$2.6 \times 10^{-14}$	$6.3 \times 10^{-14}$		$6.6 \times 10^{-17}$	32	26			

<sup>a</sup> Case A cratering rate,  $D > 10$  km [ $\text{km}^{-2} \text{year}^{-1}$ ].<sup>b</sup> Case B cratering rate,  $D > 10$  km [ $\text{km}^{-2} \text{year}^{-1}$ ].<sup>c</sup> Smith et al. (1989) cratering rates,  $D > 10$  km [ $\text{km}^{-2} \text{year}^{-1}$ ].<sup>d</sup> HTC and LPC (=NIC) cratering rates,  $D > 10$  km [ $\text{km}^{-2} \text{year}^{-1}$ ].<sup>e</sup> Case A time scale for  $D > 20$  km craters [Myr].<sup>f</sup> Case B time scale for  $D > 20$  km craters [Myr].<sup>g</sup> Case A catastrophic disruption time scale [Gyr].<sup>h</sup> Case B catastrophic disruption time scale [Gyr].<sup>i</sup> Colwell et al. (2000) catastrophic disruption time scale [Gyr].

### An exercise in numerology

Consider a comet that leaves the Kuiper Belt and becomes Neptune-crossing. Assume that it has roughly a 50% chance of being scattered outward to distant space, and a 50% chance of being scattered inward into a Uranus-crossing orbit. Only 1% of the comets actually strike planets (LD97). The same choices are offered at Uranus, Saturn, etc., so that in essence the comet is passed from control of one planet to the next, in accord with an idea put forth by Levison and Duncan (1997). So the relative number of comets crossing giant planet orbits goes as 1:2:4:8 in the order Jupiter to Neptune.

Let us also assume that comets mostly evolve from planet to planet through myriad small perturbations rather than through catastrophic close encounters. Then one expects that the ratio of impacts to the accumulated effects of perturbations will be linearly proportional to the ratio of the gravitationally enhanced physical cross section of the planet to the area of its Hill sphere. The gravitationally enhanced collision cross section is  $\sigma = \pi R_p^2 (1 + v_{esc}^2/v_\infty^2)$ . The Hill sphere radius is  $r_H = (\frac{1}{3} M_p/M_\odot)^{1/3} a$ , where  $a$  is the semi-major axis. One therefore expects that the relative chance of an impact vs scattering goes as  $R_p^2/r_H^2$ . For modest inclinations and eccentricities of comets with semimajor axes comparable to those of the planet, the random velocity of a stray body with respect to the planet is  $v_\infty \approx \sqrt{e^2 + i^2} V_{orb}$ , where  $V_{orb}$  is the circular orbital velocity of the planet. For Jupiter we have  $\sqrt{e^2 + i^2} \approx 0.34$  (Section 2), which includes the contribution made by comets captured in temporary orbits. If this factor is the same for all the giant planets, the relative impact rates would go as 1:0.62:0.14:0.18. To change the relative impact rates requires changing either the relative numbers of comets (from 1:2:4:8 to some other

pattern) or changing  $e$  and  $i$  from planet to planet. To recover the pattern found by L0, one must take  $\sqrt{e^2 + i^2}$  to vary between the planets as 0.34:0.42:0.25:0.20.

What one learns from this exercise in numerology is that (a) extremely simple considerations give a good first-order approximation to impact rates in the outer Solar System and (b) the high impact rates at Neptune quoted by L0 might reflect the cold initial conditions,  $i = 0.017$  and  $e = 0.05$ , of the specific Kuiper Belt source that LD97 considered. A more modern estimate would take both  $i$  and  $e$  to be between 0.2 and 0.4 in the Kuiper Belt, for which  $0.3 < \sqrt{e^2 + i^2} < 0.5$ . There is internal evidence in LD97 that their Neptune-encountering particles were cold. In their Fig. 4, a plot of inclinations vs perihelion distance, one sees that Neptune encounters occur with  $i \approx 0.2$  while encounters with the other three giant planets occur with  $i \approx 0.3$ . Their Fig. 6, although less clear, shows a similar trend for  $e$ . Here we will arbitrarily reduce the L0 impact rate at Neptune by a factor of 2 (i.e., in the ratio of  $i^2$ ), which is a conservative adjustment given our discussion. Even with this adjustment, it seems likely enough that we have overestimated the relative impact rates at Uranus and Neptune.

### Triton et al.

Using impact fluxes that predate the discovery of the Kuiper Belt, Smith et al. (1989) estimated Triton's surface to be no more than 1-Gyr old. Strom and co-workers (Strom et al., 1990; Croft et al., 1995) revised this age downward to less than 600 Myr. They expressed their estimate as an upper limit because they suspected that a significant fraction of the craters on Triton are of planetocentric origin. Stern and McKinnon (2000) assumed that the craters are of heliocentric origin and that the source of the comets is the

Kuiper Belt. They used LD97’s ecliptic comet flux at Neptune to deduce an average age of 100–300 Myr.

We suspect that the surfaces imaged by Voyager 2 may be younger still. Stern and McKinnon estimate that the global impact rate on Triton is currently  $\dot{N}(d > 2 \text{ km}) = 1 \times 10^{-7}/\text{year}$ . By comparison our estimates are  $\dot{N}(d > 2 \text{ km}) = 2.3 \times 10^{-7}$  per annum and  $\dot{N}(d > 2 \text{ km}) = 4.8 \times 10^{-7}$  per annum in Cases A and B, respectively. The difference between estimates derives almost entirely from Stern and McKinnon calibrating to L0’s impact rate at Jupiter. The difference is well within the range of uncertainty. If we assume a heliocentric source for the impactors, our best estimates for the nominal ages for surfaces near the apex of motion are between 60 and 350 Myr for Cases B and A, respectively. These are young but not amazingly so. However, nominal ages near the Neptune-facing meridian ( $\beta = 90^\circ$ ) are 6–40 Myr, and these are young enough to catch attention. Nominal cratering rates in the Neptune system are shown in Figs. 11 and 12.

As we have discussed in detail elsewhere (Z01), one of the puzzles of the outer Solar System is how poorly we find the predicted apex–antapex asymmetry expressed on real synchronous satellites. Triton’s exaggerated apex–antapex asymmetry only makes this disagreeable state look worse. Perhaps the meridional terrains (mostly cantaloupe) are truly younger than the rest of Triton; or impact craters may have been missed there (a possibility, as the cantaloupe terrane seems almost to have been designed as camouflage for degraded craters); or the impactors may have been mostly planetocentric bodies in prograde orbits, striking retrograde Triton more or less head on.

Neptune’s inner satellites, like those of Uranus, appear to be subject to collisional disruption on time scales shorter than the age of the Solar System. We reiterate that disruption as used here may only mean that all craters are erased, yet it might also mean disaggregation followed by reaccre-

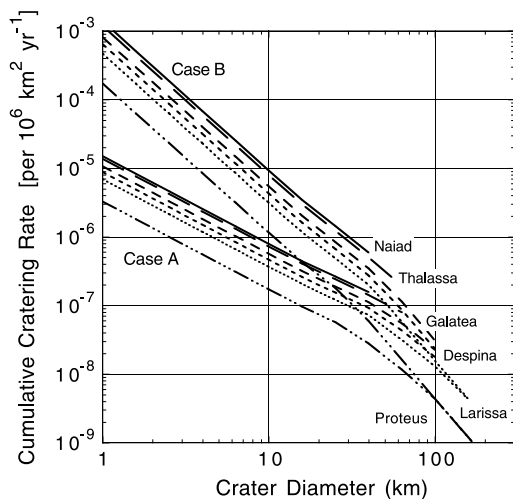


Fig. 11. Cumulative cratering rates for the Voyager inner moons of Neptune. Cases A and B are shown.

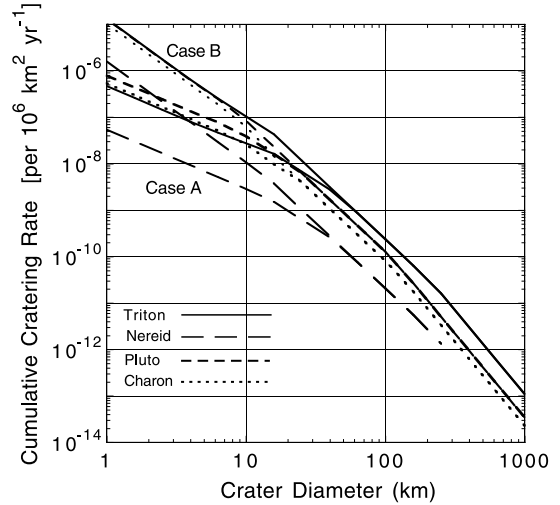


Fig. 12. Cumulative cratering rates for Triton, Nereid, Pluto, and Charon. Cases A and B are shown.

tion, or something greater still. The neptunian inner moons are generally larger and more stable than their uranian counterparts. The disruption time scales are also more unequal. We note, as we did at Uranus, that the Case B rates are both shorter and more unequal, so that in Case B the innermost satellites would seem to be destined to vanish in the near future. Case C—a truly collisional Kuiper Belt population—makes Naiad’s prospects even worse. In other words, the survival of the uranian and neptunian inner moons offers some support for the hypothesis that small comets are intrinsically rare and that the Kuiper Belt (or scattered disk) is not collisionally evolved.

### 5.5. Pluto

Pluto has to be treated separately; it was not included in LD97 nor should it have been. Nesvorný et al. (2000) estimate that the impact rate of Kuiper Belt objects on Pluto is  $\sim 7 \times 10^{-16}$  per annum per object. Using archival compilations of known Kuiper Belt orbits, W. Bottke (personal communication) estimates that the impact rate on Pluto is a little lower,  $\sim 5 \times 10^{-16}$  per annum per object. We will take the average. Trujillo et al. (2001) estimates that there are  $\sim 38,000^{+20,000}_{-15,000}$  Kuiper Belt objects with  $d > 100 \text{ km}$ . We therefore estimate an impact rate on Pluto of  $\dot{N}(d > 100 \text{ km}) = 2.3^{+2.3}_{-1.2} \times 10^{-11}$  per annum. We use our universal comet size distributions to relate this impact rate to  $d = 1.5 \text{ km}$ . These give  $\dot{N}(d > 1.5 \text{ km}) = 1 \times 10^{-6}$  and  $\dot{N}(d > 1.5 \text{ km}) = 2.6 \times 10^{-6}$  per annum for Case A and Case B, respectively. This is quite similar to the corresponding impact rate of  $\dot{N}(d > 2.4 \text{ km}) = 5.4 \times 10^{-7}$  per annum obtained by Weissman and Stern (1994) for Kuiper Belt objects. W. Bottke (personal communication) finds an average impact velocity on Pluto of 1.9 km/s, for which gravitational focusing is modest. With gravitational focusing the impact rate on Charon is 16% that on Pluto.

Our estimate is somewhat lower than the corresponding collision rate obtained by Durda and Stern (2000),  $\dot{N}(d > 2 \text{ km}) = 2.6 \times 10^{-6}$  per annum. Our Case A and Case B rates correspond to collision rates on Pluto of  $\dot{N}(d > 2 \text{ km}) = 6 \times 10^{-7}$  and  $1.2 \times 10^{-6}$  per annum, respectively. A difference between our results and Durda and Stern's is that we have taken  $v_\infty = 1.9 \text{ km/s}$ . By contrast Durda and Stern assumed a colder population with  $e = 0.2$  and  $i = 0.1$ , which implies that  $v_\infty \approx \sqrt{e^2 + i^2} V_{\text{orb}} \approx 1.06 \text{ km/s}$ ; the low  $v_\infty$  doubles the impact rate on Pluto via gravitational focusing. Durda and Stern (2000) estimate that the impact rate on Charon is  $\dot{N}(d > 2 \text{ km}) = 3.1 \times 10^{-7}$  per annum, which is only 50% higher than our Case B rate.

The net effect of the trade-off between higher impact rates and lower impact velocities is that cratering rates on Pluto and Charon are about the same as cratering rates on Triton and Europa. Our best guess is that 20-km-diameter impact craters are 5- or 6-Myr events on Pluto in either Case A or Case B. Our nominal cratering rates for Pluto and Charon are shown in Fig. 12.

## 6. Discussion

In this paper we have presented cratering rates that span the outer Solar System. By placing a heavy weight on the historical record of close encounters with Jupiter we have favored generally high impact rates, especially for comets with diameters larger than a few kilometers. In particular we have concluded that the satellite systems of Saturn, Uranus, and Neptune are not stable against collisionally induced evolution over the age of the Solar System. At the smaller scale we have reached the opposite conclusion—that comets smaller than kilometer size are relatively rare and that small primary craters are produced less frequently than one might expect. This latter conclusion is tightly based on data at Jupiter, where the result is not really in doubt, but we have attempted to show that the same paucity of small comets is allowed by crater counts on the moons of the more distant planets (yet neither is it proved).

Among the questions directly addressed by this study, it is the collisionally induced evolution of the satellite systems and the disappearance of small comets that seem most worth additional discussion. These questions may be related.

In this study we have made a weak case that comets smaller than kilometer size are rare among the current Kuiper Belt source of ecliptic comets. We have argued that crater counts in the outer Solar System do not prove that small comets are abundant at Neptune or Saturn, although (unlike at Jupiter) small comets are permitted. We have also argued that the collisional lifetimes of the uranian space-age moons are more consistent with an impacting population that lacks abundant small comets. Indeed the comet-size distribution we deduce at Jupiter gives lifetimes for the uranian satellites that are all  $\sim 2$  Gyr. The specific 2-Gyr time scale should not be taken too seriously, but that the disruption time

scales for the different satellites are all about equal is an outcome specific to the Jovian (Case A) comet-size distribution. The more nearly collisional comet-size distributions (Case B and Case C) imply that the smaller moons have much shorter collisional lifetimes than do the larger moons. Moreover, these lifetimes are quite short, typically much less than 1 Gyr. The implication is that the smaller moons are vanishing to the benefit of their larger neighbors; it becomes a puzzle that so many should exist now.

There is a view that the Kuiper Belt needs to have been collisional at its current location. The argument is that densities two or three orders of magnitude higher than they are now are needed to spawn worlds like Pluto and QB1 in situ (Stern, 1995; Kenyon, 2002). Such a thick swarm of bodies inevitably generates a lot of debris. If thereafter the Kuiper Belt evolved in a way that preserved the size-number distribution, small Kuiper Belt Objects would now be abundant. It would therefore be required that most of the small comets vanish before they reach Jupiter, and perhaps before they reach Neptune. Near Jupiter one might ask whether  $\text{CO}_2$  or  $\text{NH}_3$  vaporization could be disruptive; at greater distances one might ask the same of  $\text{CO}_2$ ,  $\text{N}_2$ , or  $\text{CH}_4$ . Comets are known to contain volatiles that can erupt beyond Saturn. Chiron is known to have been active at 13 AU and P/Halley had an outburst at 14 AU.

A second possibility is that in losing the greater part of its primordial mass the Kuiper Belt shed its smaller comets preferentially. How this might have happened is open to speculation. Perhaps the smaller fragments were carried off with the gas, leaving only the larger bodies in place. A third choice is to suggest that the larger Kuiper Belt Objects formed closer to the Sun, in rough analogy to how Neptune and Uranus may have formed near Jupiter and Saturn, only later to be scattered to greater distances (Thommes et al., 1999, 2002). Migration obviates the need for in situ collisional evolution, and so no large population of small comets need form at the Kuiper Belt's distance in the first place.

Some of the same options apply to a scattered disk. By construction the comets of the scattered disk are thrown from regions where large planets grew. It is therefore likely that they grew in a collisional environment. However the generally higher gas densities closer to the Sun and the scattering process itself offer additional opportunities for size sorting. Occultations of stars by KBOs may eventually settle the question of the population of small comets.

## Acknowledgments

This study has evolved over an astronomically long time scale through a sequence of conditionally stable drafts. Hence it has acquired many fathers. We thank W. Bottke, A. Dobrovolskis, D. Jewitt, J. Moore, C. Phillips, and H. Weaver. This work was supported by grants from NASA's Exobiology and Planetary Geology and Geophysics programs.

## Appendix: Crater diameters

Based both on laboratory experiments in wet sand and on much larger chemical explosions of known yield in known targets, Schmidt and Housen (1987) recommended two slightly inconsistent expressions for “apparent” volume and “apparent” diameter of simple craters in rock. These are equivalent to

$$V_{\text{ap}} = 0.13 \left( \frac{m_i}{\rho_t} \right)^{0.783} g^{-0.65} \left( \frac{\rho_i}{\rho_t} \right)^{0.217} v_i^{1.3} \text{ cm}^3 \quad (\text{A1})$$

for volume and

$$D_{\text{ap}} = 1.1 \left( \frac{m_i}{\rho_t} \right)^{0.26} g^{-0.22} v_i^{0.44} \left( \frac{\rho_i}{\rho_t} \right)^{0.073} \text{ cm} \quad (\text{A2})$$

for diameter. All quantities in Eq. (A1) and Eq. (A2) are to be evaluated in cgs units. In these expressions the impactor has mass  $m_i$ , density  $\rho_i$ , and velocity  $v_i$ ; surface gravity is  $g$  and target density is  $\rho_t$ . “Apparent” volume  $V_{\text{ap}}$  and “apparent” diameter  $D_{\text{ap}}$  refer to the crater volume and crater diameter measured at the plane of the original surface. Thus “apparent” volume corresponds closely to ejecta volume, but “apparent” diameter is less than the rim-to-rim diameter that one sees.

These expressions need to be supplemented by the effect of incidence angle. In ZDL98 we used the diameter expression, Eq. (A2), and we assumed that only the normal component of the impact velocity contributed to the impact, so that  $D_{\text{ap}} \propto \cos^{0.44} \theta$ , where the incidence angle is measured from the zenith. Laboratory experiments (see Melosh, 1989, p. 121) indicate that it is better to take  $V_{\text{ap}} \propto \cos \theta$ . The mean and median value of the incidence angle for isotropic velocities is  $45^\circ$ . We will assume this value unless we explicitly state otherwise.

To compare either Eq. (A1) or Eq. (A2) to what one sees requires converting “apparent” quantities to the larger observable rim-to-rim diameter. We omitted this correction in ZDL98. Here we will assume a paraboloidal crater of diameter  $D$  and depth  $\delta$ , such that the observed diameter  $D_s$  and depth  $\delta_s$  of a simple crater are related to the corresponding “apparent” values by

$$\delta_{\text{ap}} = \delta_s (D_{\text{ap}}/D_s)^2. \quad (\text{A3})$$

For simple craters the depth/diameter ratio  $\delta_s/D_s$  is constant, equal to 0.2 for Earth’s moon and the icy Galilean satellites (Schenk et al., 2003). The volume of the “apparent” crater is  $V_{\text{ap}} = \pi D_{\text{ap}}^2 \delta_{\text{ap}}/8$  and the volume of the simple crater is  $V_s = \pi D_s^2 \delta_s/8$ . By definition, the measured crater depth is equal to the sum of the apparent depth and the measured height of the rim,  $h_s$ ; i.e.,  $\delta_s = \delta_{\text{ap}} + h_s$ . Observations indicate that  $h_s/\delta_s = 0.15$  (Schenk, 1991). It follows that

$$V_{\text{ap}} = V_s (1 - h_s/\delta_s)^2. \quad (\text{A4})$$

The diameter  $D_s$  of the simple crater is given by

$$D_s = \left( \frac{8V_{\text{ap}}}{\pi} \right)^{1/3} (1 - h_s/\delta_s)^{-2/3} \left( \frac{\delta_s}{D_s} \right)^{-1/3}. \quad (\text{A5})$$

Evaluated for icy satellites in convenient units, Eq. (A5) becomes

$$D_s = 13.4(v^2/g)^{0.217} (\rho_i/\rho_t)^{0.333} \cos^{0.333} \theta d^{0.783} \text{ km}, \quad (\text{A6})$$

where  $v$  is in km/s,  $g$  in  $\text{cm/s}^2$ ,  $\rho$  in  $\text{g/cm}^3$ , and both crater diameter  $D$  and comet diameter  $d$  are in km. This expression gives craters that are about 10% smaller than what we used in ZDL98.

Equation (A6) gives the rim-to-rim crater diameter for craters smaller than  $D_c$ , the transition diameter between simple and complex craters. This transition diameter varies widely from world to world, and even between different terrains on the same world. Complex craters are broader and shallower than the corresponding simple crater. The diameter of the complex crater is often related to the diameter of the transient simple crater by an expression like

$$D = D_s (D_s/D_c)^\xi, \quad (\text{A7})$$

where the value of the exponent  $\xi$  varies among authorities but is typically on the order of  $\sim 0.13$  (e.g., McKinnon et al., 1991). For large worlds the transition diameter  $D_c$  appears to vary inversely with surface gravity and directly with target density (e.g., Melosh, 1989; Schenk, 1989). For Europa, Callisto, and Ganymede measured values of  $D_c$  range from 2 to 3 km; for these larger satellites we may take  $D_c \approx 2.5$  km (Schenk et al., 2003). The smaller icy satellites with good data—Rhea, Dione, Tethys, Ariel, Enceladus, Miranda, and Mimas—all have  $D_c$  in the range of 15 to 25 km, with no clear trend with  $g$  (Schenk, 1989). Triton, which is of intermediate size, has  $D_c \approx 6$  km (Croft et al., 1995). We will assume the same for Pluto. For the rest of the satellites we will take  $D_c = 15$  km. In all cases we will take the average incident angle  $\theta = 45^\circ$ .

## References

- Alvarellos, J., Dobrovolskis, A., Hamill, P., Zahnle, K., 2002. Orbital dynamics of Gilgamesh impact ejecta. *Icarus* 160, 108–123.
- Asphaug, E., Benz, W., 1996. Size, density, and structure of Comet Shoemaker–Levy 9 inferred from the physics of tidal breakup. *Icarus* 121, 225–248.
- Bailey, M., Clube, S.V.M., Hahn, G., Napier, W.M., Valsecchi, G.B., 1994. Hazards due to giant comets: climate and short-term catastrophism, in: Gehrel, T. (Ed.), *Hazards due to Comets and Asteroids*. Univ. of Arizona Press, Tucson, pp. 479–533.
- Bézar, B., Lellouch, E., Strobel, D., Maillard, J.-P., Drossart, P., 2002. Carbon monoxide on Jupiter: evidence for both internal and external sources. *Icarus* 159, 95–111.
- Bottke, W.F., Morbidelli, A., Jedicke, R., Petit, J.-M., Levison, H.F., Michel, P., Metcalfe, T.S., 2002. Debiased orbital and absolute magnitude distribution of the near-Earth objects. *Icarus* 156, 399–433.

- Burbine, T.H., Buchanan, P., Binzel, R., Bus, S., Hiroi, T., Hinrichs, J., Meibom, A., McCoy, T., 2001. Vesta, Vestoids, and the howardite, eucrite, diogenite group: relationships and the origin of spectral differences. *Meteoritics Planet. Sci.* 36, 761–781.
- Chapman, C.R., McKinnon, W.B., 1986. Cratering of planetary satellites, in: Burns, J.A., Matthews, M.S. (Eds.), *Satellites*, Univ. of Arizona Press, Tucson, pp. 507–553.
- Colwell, J., Esposito, L., Bundy, D., 2000. Fragmentation rates of small satellites in the outer Solar System. *J. Geophys. Res.* 105, 17589–17599.
- Croft, S.K., Kargel, J.S., Kirk, R.L., Moore, J.M., Schenk, P.M., Strom, R.G., 1995. The geology of Triton, in: Cruikshank, D.P. (Ed.), *Neptune and Triton*, Univ. of Arizona Press, Tucson, pp. 879–947.
- Dohnanyi, J.S., 1972. Interplanetary objects in review: statistics of their masses and dynamics. *Icarus* 17, 1–48.
- Donnison, J.R., 1986. The distribution of cometary magnitudes. *Astron. Astrophys.* 167, 359–363.
- Drake, M.J., 2001. The eucrite/Vesta story. *Meteoritics Planet. Sci.* 36, 501–513.
- Duncan, M.J., Levison, H.F., 1997. A scattered comet disk and the origin of Jupiter family comets. *Science* 276, 1670–1672.
- Duncan, M., Quinn, T., Tremaine, S., 1988. The origin of short-period comets. *Astrophys. J.* 328, L69–L73.
- Durda, D.D., Stern, S.A., 2000. Collision rates in the present-day Kuiper Belt and Centaur regions: applications to surface activation and modification on comets, Kuiper Belt objects, Centaurs and Pluto–Charon. *Icarus* 145, 220–229.
- Everhart, E., 1967. Intrinsic distributions of cometary perihelia and magnitudes. *Astron. J.* 72, 1002–1011.
- Fernandez, J.A., Tancredi, G., Rickman, H., Licandro, J., 1999. The population, magnitudes, and sizes of Jupiter family comets. *Astron. Astrophys.* 352, 327–340.
- Fernandez, Y.R., Jewitt, D.C., Sheppard, S.S., 2002. Thermal properties of Centaurs Asbolus and Chiron. *Astron. J.* 123, 1050–1055.
- Gladman, B., Kavelaars, J.J., Petit, J.-M., Morbidelli, A., Holman, M.J., Lored, T., 2001. The structure of the Kuiper Belt: size distribution and radial extent. *Astron. J.* 122, 1051–1066.
- Greeley, R., Heiner, S., Klemaszewski, J., 2001. Geology of Lofn crater. Callisto. *J. Geophys. Res.* 106, 3261–3273.
- Hamilton, D., Burns, J., 1994. Saturn's E Ring: self-sustained, naturally. *Science* 265, 550–553.
- Harrington, J., de Pater, I., Brecht, S., Deming, D., Meadows, V., Nicholson, P., Zahnle, K., 2003. Lessons from Shoemaker–Levy 9 about Jupiter and planetary impacts, in: Bagenol, F., MacKinnon, W. (Eds.), *Jupiter II*, Cambridge University Press.
- Holman, M.J., Wisdom, J., 1993. Dynamical stability in the outer Solar System and the delivery of short-period comets. *Astron. J.* 105, 1987–1999.
- Horedt, G.P., Neukum, G., 1984. Cratering rate over the surface of a synchronous satellite. *Icarus* 60, 710–717.
- Hughes, D.W., 1988. Cometary magnitude distribution and the ratio between the numbers of long- and short-period comets. *Icarus* 73, 149–162.
- Ivanov, B.A., Neukum, G., De Niem, D., 1998. Cometary impact rates on jovian satellites: questions. *Lunar Planet. Sci.* 29, 1769 (abstract).
- Jewitt, D., Trujillo, C.A., Luu, J.X., 2000. Population and size distribution of small jovian trojan asteroids. *Astron. J.* 120, 1140–1147.
- Kary, D.M., Dones, L., 1996. Capture statistics of short-period comets: implications for Comet D/Shoemaker–Levy 9. *Icarus* 121, 207–224.
- Kenyon, S.J., 2002. Planet formation in the outer Solar System. *Publ. Astron. Soc. Pac.* 114, 265–283.
- Kidger, M., 1997. <http://galileo.ivv.nasa.gov/comet/news66.html>.
- Kresak, L., Pittich, E.M., 1978. The intrinsic number density of active long-period comets in the inner Solar System. *Astron. Inst. Czech. Bull.* 29, 299–309.
- Kronk, G.W., 1984. *Comets, a Descriptive Catalog*. Enslow Publishers, Hillside, NJ and Aldershot, U.K..
- Kronk, G.W., 2001. *Cometography*. Vol. 1. Cambridge University Press.
- Kronk, G.W., 2003. *Cometography*. Vol. 2. Cambridge University Press.
- Lellouch, E., Bézard, B., Moreno, R., Bockelée-Morvan, D., Colum, P., Crovisier, J., Festou, M., Gautier, D., Marten, A., Paubert, G., 1997. Carbon monoxide in Jupiter after the impact of Comet Shoemaker–Levy 9. *Planet. Space Sci.* 45, 1203–1212.
- Lellouch, E., Bézard, B., Moses, J., Davis, G., Drossart, P., Feuchtgruber, H., Bergin, E., Moreno, R., Encrenaz, T., 2002. The origin of water vapor and carbon dioxide in Jupiter's stratosphere. *Icarus* 159, 112–131.
- Levison, H.F., 1996. Comet taxonomy, in: T.W. Rettig, J.M. Hahn (Eds.), *Completing the Inventory of the Solar System*, Astron. Soc. Pac. Conf. Proc. 107, 173–191.
- Levison, H., Duncan, M., 1997. From the Kuiper Belt to Jupiter-family comets: the spatial distribution of ecliptic comets. *Icarus* 127, 13–32.
- Levison, H.F., Shoemaker, E.M., Shoemaker, C.S., 1997. Dynamical evolution of Jupiter's Trojan asteroids. *Nature* 385, 42–44.
- Levison, H.F., Duncan, M.J., Zahnle, K., Holman, M., Dones, L., 2000. Planetary impact rates from ecliptic comets. *Icarus* 143, 415–420.
- Levison, H.F., Morbidelli, A., Dones, L., Jedicke, R., Weigert, P.A., Bottke, W.F., 2002. The mass suicide of Oort cloud comets. *Science* 296, 2212–2215.
- Lissauer, J.J., Squyres, S.W., Hartmann, W.K., 1988. Bombardment history of the Saturn system. *J. Geophys. Res.* 93, 13776–13804.
- Lowry, S.C., Fitzsimmons, A., Collander-Brown, S., 2003. CCD photometry of distant comets III. *Astron. Astrophys.* 397, 329–343.
- Marzari, F., Dotto, E., Davis, D.R., Weidenschilling, S.J., Vanzani, V., 1998. Modelling the disruption and reaccumulation of Miranda. *Astron. Astrophys.* 333, 1082–1091.
- McGhee, C.A., Nicholson, P.D., French, R.G., Hall, K.J., 2001. HST Observations of saturnian satellites during the 1995 ring plane crossings. *Icarus* 152, 282–315.
- McKinnon, W.B., Chapman, C.R., Housen, K.R., 1991. Cratering of the uranian satellites, in: Bergstrahl, J.T., Miner, E.D., Matthews, M.S. (Eds.), *Uranus*, Univ. of Arizona Press, Tucson, pp. 629–692.
- Melosh, H.J., 1989. *Impact Cratering: A Geological Process*. Oxford Univ. Press, New York.
- Moore, J., 2003. in: Bagenol, F., MacKinnon, W. (Eds.), *Jupiter II*, Cambridge University Press.
- Nakamura, T., Kurahashi, H., 1998. Collisional probability of periodic comets with the terrestrial planets. *Astron. J.* 115, 848–854.
- Nakamura, T., Yoshikawa, M., 1995. Close encounters and collisions of short-period comets with Jupiter and its satellites. *Icarus* 116, 113–130.
- Nesvorný, D., Roig, F., Ferraz-Mello, S., 2000. Close approaches of trans-neptunian objects to Pluto have left observable signatures on their orbital distribution. *Astron. J.* 119, 953–969.
- Nesvorný, D., Alvarillos, J.L.A., Dones, L., Levison, H.F., 2003. Orbital and collisional evolution of the irregular satellites. *Astron. J.*, in press.
- Nicholson, P.D., Hamilton, D.P., Matthews, K., Yoder, C.F., 1992. New observations of Saturn's coorbital satellites. *Icarus* 100, 464–484.
- Plescia, J.B., 1987a. Geologic terrains and crater frequencies on Ariel. *Nature* 327, 201–204.
- Plescia, J.B., and others, 1987b. Cratering history of Miranda: implication for geologic processes. *Icarus* 73, 442–461.
- Plescia, J.B., 1989. Cratering history of the uranian satellites: Umbriel, Titania, and Oberon. *J. Geophys. Res.* 92, 14918–14932.
- Rahe, J., Vanysek, V., Weissman, P.R., 1994. Properties of cometary nuclei, in: Gehrels, T. (Ed.), *Hazards due to Comets and Asteroids*, Univ. of Arizona Press, Tucson, pp. 597–634.
- Rogers, J.H., 1995. *The Giant Planet Jupiter*. Cambridge Univ. Press, Cambridge, UK.
- Rogers, J.H., 1996. The comet collision with Jupiter: the visible scars. *J. Brit. Astron. Assoc.* 106, 125–150.
- Safronov, V.S., 1972. Evolution of the Protoplanetary Cloud and Formation of the Earth and the Planets. *NASA Tech. Transl. F-677*.
- Schenk, P.M., 1989. Crater formation and modification on the icy satellites of Uranus and Saturn: depth/diameter and central peak occurrence. *J. Geophys. Res.* 94, 3813–3832.

- Schenk, P.M., 1991. Complex craters on Ganymede and Callisto. *J. Geophys. Res.* 96, 15634–15664.
- Schenk, P.M., Sobieszczyk, S., 1999. Cratering asymmetries on Ganymede and Triton: from the sublime to the ridiculous. *Bull. Am. Astron. Soc.* 31, 1182.
- Schenk, P.M., Chapman, C., Moore, J., Zahnle, K., 2003. Ages and Interiors: the cratering record of the Galilean satellites, in: F. Bagenal, W. McKinnon (Eds.), *Jupiter: Planet, Magnetosphere, Satellites, and Magnetosphere*, Cambridge Univ. Press, Cambridge, UK, pp.
- Schmidt, R.M., Housen, K.R., 1987. Some recent advances in the scaling of impact and explosive cratering. *Int. J. Impact Eng.* 5, 543–560.
- Scotti, J., Melosh, H.J., 1993. Estimate of the size of Comet Shoemaker–Levy 9 from a tidal breakup model. *Nature* 365, 733–735.
- Sekanina, Z., Yeomans, D.K., 1985. Orbital motion, nuclear precession, and splitting of periodic comet Brooks 2. *Astron. J.* 90, 2335–2352.
- Sheppard, S., Jewitt, D., Trujillo, C., Brown, M., Ashley, M., 2000. A wide-field CCD survey for Centaurs and Kuiper Belt objects. *Astron. J.* 120, 2687–2699.
- Shoemaker, E.M., Wolfe, R.A., 1982. Cratering timescales for the Galilean satellites, in: Morrison, D. (Ed.), *Satellites of Jupiter*, Univ. of Arizona Press, Tucson, pp. 277–339.
- Shoemaker, E.M., Shoemaker, C.S., Wolfe, R.A., 1989. Trojan asteroids: populations, dynamical structure, and origin of the L4 and L5 swarms, in: Binzel, R.P., Gehrels, T., Matthews, M.S. (Eds.), *Asteroids II*, Univ. of Arizona Press, Tucson, pp. 487–523.
- Shoemaker, E.M., Weissman, P.R., Shoemaker, C.S., 1994. The flux of periodic comets near Earth, in: T. Gehrels (Eds.), *Hazards due to Comets and Asteroids*, Univ. of Arizona Press, Tucson, pp. 313–335.
- Showman, A., Malhotra, R., 1997. Tidal evolution of the Laplace resonance and the resurfacing of Ganymede. *Icarus* 127, 93–111.
- Smith, B.A., and 32 colleagues, 1981. Encounter with Saturn: Voyager 1 imaging results. *Science* 212, 163–190.
- Smith, B.A., and 32 colleagues, 1982. A new look at the Saturn system: the Voyager 2 images. *Science* 215, 504–537.
- Smith, B.A., and 32 colleagues, 1986. Voyager 2 in the uranian system: imaging science results. *Science* 233, 43–64.
- Smith, B.A., and 32 colleagues, 1989. Voyager 2 in the neptunian system: imaging science results. *Science* 246, 1422–1449.
- Spohn, T., Breuer, D., 1998. Implications from Galileo observations on the interior structure and evolution of the Galilean satellites, in: Celnikier, L., Tran Thanh Van, J. (Eds.), *Planetary Systems: The Long View*, Editions Frontieres Gif-sur-Yvette, France, pp. 135–144.
- Steel, D.I., 1993. Collisions in the Solar System—V. Terrestrial impact probabilities for parabolic comets. *Mon. Not. R. Astron. Soc.* 264, 813–823.
- Stern, S.A., 1995. Collisional time scales in the Kuiper disk and their implications. *Astron. J.* 110, 856–868.
- Stern, S.A., McKinnon, W.B., 2000. Triton's surface image and impactor population revisited in light of Kuiper Belt fluxes: evidence for small Kuiper Belt objects and recent geological activity. *Astron. J.* 119, 945–952.
- Stevenson, D.J., 2001. Mars core and magnetism. *Nature* 412, 214–219.
- Strom, R.G., 1987. The Solar System cratering record: Voyager 2 results at Uranus and implications for the origin of impacting objects. *Icarus* 70, 517–535.
- Strom, R.A., Croft, S.K., Boyce, J.M., 1990. The impact cratering record on Triton. *Science* 250, 437–439.
- Tabe, I., Watanabe, J., Jimbo, M., 1997. Discovery of a possible impact spot on Jupiter recorded in 1690. *Publ. Astron. Soc. Jpn.* 49, L1–L5.
- Tanaka, H., Inaba, S., Nakazawa, K., 1996. Steady-state size distribution for the self-similar cascade. *Icarus* 123, 450–455.
- Tancredi, G., Fernandez, J.A., Rickman, H., Licandro, J., 2000. A catalog of observed nuclear magnitudes of Jupiter family comets. *Astron. Astrophys. Supp.* 146, 73–90.
- Thommes, E.W., Duncan, M.J., Levison, H.F., 1999. The formation of Uranus and Neptune in the Jupiter–Saturn region of the Solar System. *Nature* 402, 635–638.
- Thommes, E.W., Duncan, M.J., Levison, H.F., 2002. The formation of Uranus and Neptune among Jupiter and Saturn. *Astron. J.* 123, 2862–2883.
- Tremaine, S., Dones, L., 1993. On the statistical distribution of massive impactors. *Icarus* 106, 335–341.
- Trujillo, C.A., Jewitt, D.C., Luu, J.X., 2001. Properties of the trans-neptunian belt: statistics from the Canada–France–Hawaii Telescope Survey. *Astron. J.* 122, 457–473.
- Weissman, P.R., 1989. The impact history of the Solar System: implications for the origin of atmospheres, in: Atreya, S.K., Pollack, J.B., Matthews, M.S. (Eds.), *Origin and Evolution of Planetary and Satellite Atmospheres*, Univ. of Arizona Press, Tucson, pp. 230–267.
- Weissman, P.R., 1991. Dynamical history of the Oort cloud, in: Newburn, R.L., Neugebauer, M., Rahe, J. (Eds.), *Comets in the Post-Halley Era*, Kluwer, Dordrecht, pp. 463–486.
- Weissman, P.R., Levison, H., 1997. The population of the trans-neptunian region: the Pluto–Charon environment, in: Stern, S.A., Tholen, D.J. (Eds.), *Pluto and Charon*, Univ. of Arizona Press, Tucson, pp. 559–604.
- Weissman, P.R., Stern, S.A., 1994. The impactor flux in the Pluto–Charon system. *Icarus* 111, 378–386.
- Wiegert, P.A., Tremaine, S., 1999. The evolution of long period comets. *Icarus* 137, 84–121.
- Williams, D.R., Wetherill, G.W., 1994. Size distribution of collisionally evolved asteroidal populations: analytical solution for self-similar collision cascades. *Icarus* 107, 117–128.
- Yoder, C.F., Synnott, S.P., Salo, H., 1989. Orbits and masses of Saturn's co-orbiting satellites, Janus and Epimetheus. *Astron. J.* 98, 1875–1889.
- Zahnle, K., 1996. Dynamics and chemistry of SL9 plumes, in: Noll, K., Weaver, H.A., Feldman, P.D. (Eds.), *The Impact of SL9 with Jupiter*, IAU Conference Proceedings, Cambridge Univ. Press, Cambridge UK, pp. 183–212.
- Zahnle, K., Dones, L., Levison, H., 1998. Cratering rates on the Galilean satellites. *Icarus* 136, 202–222.
- Zahnle, K., Schenk, P., Sobieszczyk, S., Dones, L., Levison, H., 2001. Differential cratering of synchronously rotating satellites by ecliptic comets. *Icarus* 153, 111–129.